UNIVERSITY *of* York

White Rose
university consortium
Universities of Leeds, Sheffield & York

eprints@whiterose.ac.uk
https://eprints.whiterose.ac.uk/

Chemical Engineering Journal

Tailored design of graphitic biochar for high-efficiency and chemical-free microwave-assisted removal of refractory organic contaminants
--Manuscript Draft--

Corresponding Author:	Daniel CW Tsang, PhD Hong Kong Polytechnic University Hong Kong, HONG KONG
First Author:	Yuqing Sun, PhD
Order of Authors:	Yuqing Sun, PhD
	Iris KM Yu, PhD
	Daniel CW Tsang, PhD
	Jiajun Fan, PhD
	James H Clark, PhD
	Gang Luo, PhD
	Shicheng Zhang, PhD
	Eakalak Khan, PhD
	Nigel JD Graham, PhD

Abstract:	Energy-saving, chemical-free, and high-efficiency microwave (MW)-assisted water treatment can be greatly facilitated via tailored design of an economical, sustainable, and 'green' carbonaceous catalyst. Various biochars (BC) were pyrolyzed from two lignocellulosic waste biomasses, oak (O) and apple tree (A), at high temperature (900 °C) and under different gases (N2 and CO2). The holistic characterization by advanced spectroscopic techniques demonstrated that CO2 pyrolysis of feedstock with more lignin (i.e., oak), produced biochar with increased aromaticity and degree of carbonization. CO2 modification created a hierarchical porous structure, improved surface hydrophilicity, polarity, and acidity, and provided higher densities of near-surface functionalities of the biochar. Without MW irradiation, ABC-900C (1 g L−1) provided the highest adsorption (52.6%, 1 min) of 2,4-dichlorophenoxy acetic acid (2,4-D) ascribed to large specific surface area, high micropore content, appropriate pore size, and abundant active groups. OBC-900C (1 g L−1) enabled significantly increased 2,4-D removal (81.6%, 1 min) under MW irradiation (90 °C) in contrast with an oil bath (55.7%, 90 °C, 1 min) and room temperature (33.9%, 1 min) conditions, due to its highest graphitization degree and medium-developed microporous structure. The MW-induced thermal effect formed "hotspots" on the biochar surface as evidenced by elevated temperature of the bulk solution and lowered energy consumption of the MW reactor in the presence of OBC-900C, compared to those of the other biochars. The scavenging tests suggested that the generation of highly oxidative hydroxyl (•OH), anionic superoxide (O2•−), and singlet oxygen (1O2) radicals contributed to the removal of 2,4-D. This study demonstrated that biochar with customized structure and high organic adsorption capacity can act as an effective MW absorber suitable for rapid and improved removal of toxic organics.

Response to Reviewers:	Dear Prof. Gao, We sincerely appreciate the reviewers' and your constructive comments on our manuscript (CEJ-D-20-06099). The comments and suggestions have helped us to improve our manuscript and stimulate new thoughts for our ongoing studies. You can find the point-by-point list of our responses to the comments and the corresponding changes in this document. The revisions of our manuscript are highlighted in red colour

for your reference. We confirm that the figures and tables in this revised manuscript are the original work of the authors.

We hope the revised manuscript meets the criteria for publication in Chemical Engineering Journal. Thank you very much again and we look forward to hearing from you soon.

Best Wishes,
Dan (on behalf of co-authors)

THE HONG KONG
POLYTECHNIC UNIVERSITY
香港理工大學

Department of Civil and Environmental Engineering
土木及環境工程學系

香港 九龍 紅磡
Hung Hom, Kowloon, Hong Kong
Tel (852) 2766 6045 Fax (852) 2334 6389
Website www.polyu.edu.hk

16 April 2020

Dear Editor,

Attached please find our manuscript entitled "Tailored design of graphitic biochar for high-efficiency and chemical-free microwave-assisted removal of refractory organic contaminants", which is submitted for publication as an original research paper. This manuscript contains 4872 words, 8 figures, and 1 table in the text excluding references. We believe that the scientific merits and environmental significance of our manuscript fit well into the scope of *Chemical Engineering Journal*.

Significance and Novelty:

- In this study, we demonstrated that CO_2 pyrolysis of feedstock (oak tree) with highger lignin content produced biochar (OBC-900C) with a hierarchical porous structure, improved surface hydrophilicity, polarity, and surface functionalities.

- The OBC-900C (1 g L^{-1}) enabled significantly increased 2,4-dichlorophenoxy acetic acid (2,4-D) removal (81.6%, 1 min) under microwave (MW) irradiation in contrast with an oil bath (55.7%, 1 min) and room temperature (33.9%, 1 min) conditions, owing to its high MW absorption and 2,4-D adsorption capacities ascribed to high graphitization degree and medium-developed microporous structure.

- The MW-induced thermal effect formed "hot spots" on the biochar surface and generated highly oxidative hydroxyl ($^{\bullet}OH$), anionic superoxide ($O_2^{\bullet-}$), and singlet oxygen ($^1O_2$) radicals contributing to the removal of 2,4-D.

Neither the entire paper nor any part of its content has been published elsewhere, and it is not being submitted to any other journal. This submission is approved by all authors, and we declare that there is no conflict of interest regarding its publication. We sincerely appreciate your kind consideration and look forward to hearing from you.

Best Wishes,

Dan Tsang, PhD, CEnv, BEng, PG Dip (Tert Tchg)
Associate Professor, Programme Leader (EOSH)
Department of Civil and Environmental Engineering,
Hong Kong Polytechnic University,
Hung Hom, Kowloon, Hong Kong
https://www.scopus.com/authid/detail.uri?authorId=12760921200
http://www.polyu.edu.hk/cee/~dan_tsang/

THE HONG KONG
POLYTECHNIC UNIVERSITY
香港理工大學

Department of Civil and Environmental Engineering
土木及環境工程學系

Suggested Reviewers:

First Name*	Bingcai
Middle Initial	
Last Name*	Pan
Academic Degree(s)	PhD
Position	Professor
Department*	Research Center for Environmental Nanotechnology
Institution*	Nanjing University
E-mail Address*	bcpan@nju.edu.cn
Reason*	Expert at solid catalyst

First Name*	Kevin
Middle Initial	
Last Name*	Wu
Academic Degree(s)	PhD
Position	Professor
Department*	Department of Chemical Engineering
Institution*	National Taiwan University
E-mail Address*	kevinwu@ntu.edu.tw
Reason*	Expert at solid catalyst

First Name*	Bin
Middle Initial	
Last Name*	Gao
Academic Degree(s)	PhD
Position	Professor
Department*	Department of Agricultural and Biological Engineering
Institution*	University of Florida
E-mail Address*	bg55@ufl.edu
Reason*	Expert at engineered biochar

Dear Prof. Gao,

We sincerely appreciate the reviewers' and your constructive comments on our manuscript (CEJ-D-20-06099). The comments and suggestions have helped us to improve our manuscript and stimulate new thoughts for our ongoing studies. You can find the point-by-point list of our responses to the comments and the corresponding changes in this document. The revisions of our manuscript are highlighted in red colour for your reference. We confirm that the figures and tables in this revised manuscript are the original work of the authors.

We hope the revised manuscript meets the criteria for publication in *Chemical Engineering Journal.* Thank you very much again and we look forward to hearing from you soon.

Best Wishes,
Dan (on behalf of co-authors)

Reviewer # 1
Sun and co-authors test the efficacy of high temperature (900 C) biochars for the sorption and degradation of 2,4-dichlorophenoxy acetic acid (2,4-D) - a model organic contaminant - by microwave-assisted treatment. The authors find that a char produced from oak wood in the presence of CO2 during pyrolysis markedly enhances 2,4-D removal from aqueous solution, and propose that biochar may be a cost-effective alternative to other catalysts (such as metal-based catalysts) in the treatment of organic contaminants in water. I find the manuscript to be scientifically sound, generally well-written, and a good fit for publication in Chemical Engineering Journal.
Response: Many thanks for your kind support. We revised the manuscript according to your constructive suggestions and thoughtful comments as follows.

Following are some thoughts and recommendations that I hope will help the authors in revising their manuscript:
1. Page 2, Line 4: "…more near-surface functionalities of the biochar." The language is vague here - do you mean higher surface functional group densities/concentrations, or a more diverse group of functionalities at the surface?
Response: We revised this sentence for clarity as suggested (Page 2, line 1).

2. Page 2, Line 7: The authors give a reasonable explanation (Page 5, Lines 4-14) about why 2,4-D was used - that it is common and has a non-trivial toxicity. However, with only testing one model organic compound, how applicable are the general results of this study, the use of MW assisted degradation for organics? I would have liked to have seen a few more tests of a broader range of model organic contaminants, to confirm that the approach the authors propose is widely useful.
Response: As suggested, we acknowledged the need of testing with different organic compounds as a future research direction of MW-assisted biochar-catalyzed degradation in the revised manuscript (Page 17, line 19), because we had limited access to the laboratory and could not conduct a large amount of additional experiments due to the COVID-19 pandemic.

3. Page 4, Line 58: Are the trace amounts of transition metals in the biochars a concern in terms of leachability / toxicity? It would have been interesting to see the results of a sequential extraction for metals (e.g., Tessier et al., 1979).
Response: In view of your comments, we clarified in the revised manuscript (Page 7, line 20-21) that only one type of transition metal (*i.e.*, Fe) with trace amount (*i.e.*, 1-2 *wt.%*) was tested

in all the four types of biochars (Table 1) and that no leaching of metals, organics, or nutrients was detected under all the experimental conditions of this study.

4. Page 7, Lines12-19: Why was a loading of 20 mg biochar in 20 mL of solution chosen? The efficiency of removal depends on this loading, and a test as a function of loading would have been helpful to optimize the system.
Response: As suggested, we explained the reason for choosing this biochar loading in the revised manuscript (Page 7, line 8-10).

5. Page 7, Lines 31-34: Perhaps tell the reader here that 2,4-D is being quantified using HPLC.
Response: Revised as suggested (Page 7, line 15).

6. Page 8, Lines 4-49: There is not a citation for these methods of extraction and quantification. Did the authors develop this method themselves, or based on existing or similar extraction / quantification methods for 2,4-D. Later it is discussed that potential degradation compounds of 2,4-D are not detected, which could be an artifact of the HPLC method used (mobile phase, column temperature, time of elution, etc.).
Response: As suggested, references were provided for the methods used for extraction and quantification of 2,4-D in the revised manuscript (Page 8, line 7, 9, 13, 15).

7. Page 9, Lines 43-46: "CO_2 may have acidified the biochars via the creation of more near-surface oxygen-containing functional groups." Do your XPS data (and to some extent, FTIR data) support this conclusion? If so, I'd be firmer on this point (e.g,. Page 10, Lines 48-53).
Response: XPS data were used to support this conclusion and we clarified this in the revised manuscript (Page 9, line 22-23).

8. Page 11, Lines 53-56: FTIR does not identify "oxygen-containing functional groups…on the biochar surface". IR penetrates the sample significantly, and is more of a bulk technique that shows the average bonding environment (for example, of C in this case). IR analyses can be done as a function of solution pH to identify proton-active functional groups - and even their pKa's in some instances - but this is rarely done. Change the language here.
Response: Thanks again and we revised the discussion accordingly (Page 12, line 3, 5-7).

9. Page 12, Lines 55-58: Perhaps soften to "…by biochar was LIKELY a result of electrostatic…" The authors propose reasonable hypotheses about the mechanisms of adsorption, but these are not tested.
Response: We agree with you and revised the text as suggested (Page 13, line 10).

10. Pages 13-14: The authors provide a clear comparison of how the two different feedstock biomasses, N2 vs. CO2, and even pyrolysis temperature impact the efficiency of a biochar using MW for 2,4-D treatment. To make this paper more useful, can the authors provide a few sentences in the discussion and/or conclusions about feedstocks and/or pyrolysis conditions that might be most promising in MW applications? I realize that there is more optimization work to be done (a fact the authors might also mention), but some "take home" guidance would be helpful.
Response: As suggested, in view of the promising results of this proof-of-concept study, we considered optimization of feedstock type and pyrolytic conditions as a future research

direction and revised the text as suggested (Page 17, line 20-21).

11. Page 15, Lines 19-22: I assume the 10% 2,4-D recovery was measured using HPLC. In case the HPLC method was not capturing all of the degradation products, was the bulk TOC concentration at all helpful? That is, was the TOC recovery on par with the initial 2,4-D concentration in the experiment?
Response: The extraction/desorption of the reacted biochars was conducted using different organic solvents, we attempted to compare the TOC concentrations as suggested but the minor differences in the bulk solutions (especially after dilution) could not accurately demonstrate the existence of 2,4-D or its degradation products.

12. Page 15, Lines 54-56: Do the authors have any suggestions about how to regenerate OBC-900C (or more generally, a biochar) for reuse in MW applications?
Response: We proposed two regeneration methods as suggested (Page 16, line 20-22).

Reviewer #2
In this paper, the authors fabricated a series of biochars produced from two feedstock under N2/CO2 atmosphere, and used them for the microwave-assisted removal of 2,4-D. This paper is well designed with detailed characterization of materials and adequate study for the underlying mechanisms. The only doubt is how to confirm the existence of degradation process with microwave, and more experiments might be needed to clarify the main results.
Response: Many thanks for your constructive suggestions. We added more experimental results and additional discussion on our coherent findings to further improve our manuscript based on your valuable comments and thoughtful suggestions as follows.

Specific comment:
1. In my opinion, it was important to study the degradation process of 2,4-D during its removal, although it might be hard due to the strong entrapment of possible by-products. Enlarging the concentration of 2,4-D or using some other extraction reagents for the spent biochars might be helpful to identify the possible by-products. If there is no direct evidence, it is hard to conclude that the degradation process happened due to the similar TOC and pollutant removal rate. It is possible that merely sorption process occurred and the microwave only facilitated the dispersion process or the formation of surface sorption sites on the biochars?
Response: In our preliminary experiments, much higher (500 mg L^{-1}) or lower (10 mg L^{-1}) initial 2,4-D concentrations and different biochar loadings (1 and 2.5 g L^{-1}) were also tested for adsorption-desorption of 2,4-D by different organic solvents (methanol, ethanol, hexane, acetonitrile, and DMSO). However, it was noteworthy that the 2,4-D recoveries were all below 50%. Furthermore, we affirmed that radicals were generated only in the MW system (Page 15, line 2-5) and that these radicals were able to degrade 2,4-D. In our upcoming studies after the COVID-19 pandemic, we will design more comprehensive experiments and go about other experimental-computational approaches to further prove and quantify the degradation of 2,4-D in the MW/biochar system (Page 16, line 8-13).

2. If the organic pollutant is completely degraded to CO2 and H2O, there might be some Cl- left in the solution. It might be helpful to detect the soluble Cl- concentration to confirm the degradation process?
Response: As suggested, according to the latest report (Li et al., 2020, [56]), the dechlorination

rate of 2,4-D was correlated to the degradation efficiency of 2,4-D when 2,4-D was completely mineralized into CO_2 and H_2O (*viz.* radical + 2,4-D → intermediates → CO_2 + H_2O + Cl^-). We revised the manuscript accordingly (Page 16, line 8-13) and would detect the released Cl^- concentration after reaction in our future studies after the COVID-19 pandemic.

3. EPR analysis can be added to determine the free radicals during the removal process in order to further confirm the degradation process. It might also be necessary to provide the control experiment for the organic scavengers, which means only mixing organic scavenger with biochar and organic pollutants at 90°C. This can help to confirm the roles of radicals for the degradation instead of competing the sorption sites on biochar since these scavengers was organic compounds, which might change the sorption process of biochar.

Response: The EPR analysis of radicals requires sample testing immediately after reaction, yet we cannot have an immediate access to EPR (in a commercial lab) right after conducting the MW experiments in our lab. Nevertheless, we added more experimental results and explanation (Page 15, line 2-5) reaffirming that these additional organic scavengers did not affect 2,4-D adsorption by the biochars and that the radicals were only generated in the MW system.

4. The characterization of biochars is detailed and sufficient, but some conclusions need further consideration. E.g., OBC had higher aromatic peaks than ABC, but the difference between N2 and CO2 was hard to be identified in the FTIR analysis, especially considering the FTIR analysis might not be a suitable quantitative approach?

Response: The difference in contents of oxygen-containing functional groups was identified by XPS analysis (Page 12, line 3-4; Fig.4). The limitation of FTIR analysis was clarified in the revised manuscript (Page 12, line 5-7) thanks to your comments.

5. Similar to comment 4, XPS results showed the change of aromatic C=C and aromatic Π-Π* of different biochars, but the alternation is limited. It might not be precise to demonstrate the difference between biochars of two feedstock with such little gap, especially when it comes from peak-fitting. Besides, if aromatic C=C and aromatic Π-Π* both represented the degrees of aromatic rings, why it showed contrasting transition with two feedstock (i.e. oak tree had higher C=C but lower Π-Π* comparing with apple tree)?

Response: The limitation of XPS analysis was clarified in the revised manuscript (Page 12, line 11-13), and the areas of these two peaks corresponded to the content of aromatic C=C on biochar surface and the density of π–π* transition in aromatic rings of biochar, respectively. The text was revised for clarity as suggested (Page 12, line 8).

6. The reusability of biochars declined noticeably after each cycle and "popcorn effect" might be the main reason according to the author's words, which was possible, but another possible explanation of this result is the occupation of sorption sites after each cycle. So, the author can evaluate the reusability of biochar at 90°C with oil bath without microwave to exclude this possibility.

Response: We agree with you and added this possibility in the revised manuscript (Page 16, line 16-18). However, the 2,4-D adsorption capacity of biochar under MW condition might not be equivalent to that of oil bath [21], limiting the relevance of reusability test with oil bath.

7. 90 oC in the Fig.5 needs revise.

Response: Revised as suggested (Fig.5).

Graphical abstract
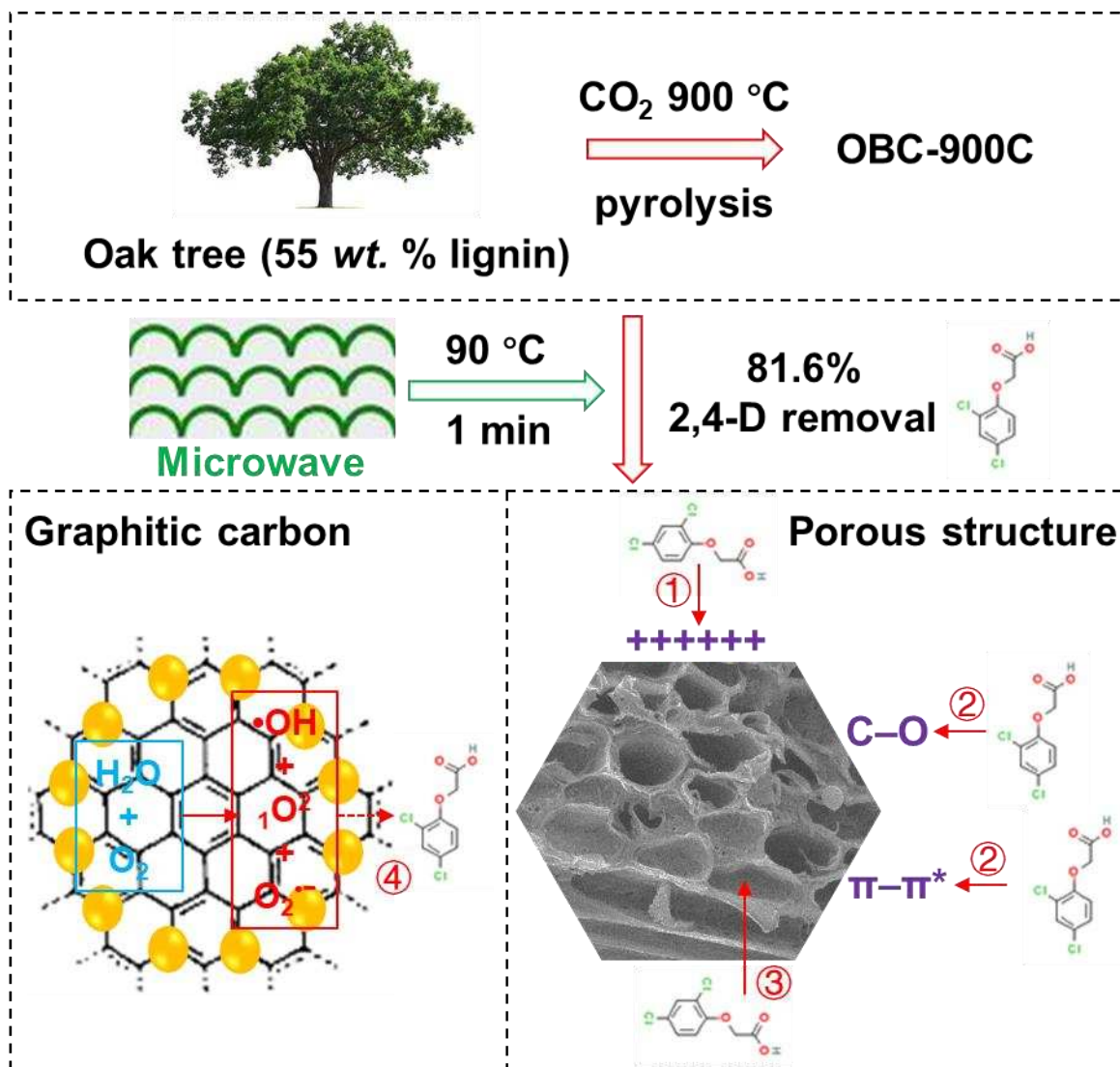
① **Electrostatic interaction** ③ **Diffusion into inner pores**
② **Chemical adsorption** ④ **Possible degradation** "Hot spots"

Highlights

- CO_2-pyrolyzed lignin-rich oak at 900 °C produced highly graphitic, porous OBC-900C

- OBC-900C exhibited high microwave (MW) absorption and 2,4-D adsorption capacities

- MW irradiation at 90 °C significantly promoted 2,4-D removal by OBC-900C

- MW-induced thermal effect generated "hot spots" and various radicals for pollutant degradation

Tailored design of graphitic biochar for high-efficiency and chemical-free microwave-assisted removal of refractory organic contaminants

Yuqing Sun [a], Iris K.M. Yu [b,c], Daniel C.W. Tsang [a,*], Jiajun Fan [b], James H. Clark [b,d], Gang Luo [d], Shicheng Zhang [d], Eakalak Khan [e], Nigel J.D. Graham [f]

[a] Department of Civil and Environmental Engineering, The Hong Kong Polytechnic University, Hung Hom, Kowloon, Hong Kong, China.

[b] Green Chemistry Centre of Excellence, Department of Chemistry, University of York, York, YO10 5DD, UK.

[c] Department of Chemistry and Catalysis Research Center, Technische Universität München, Lichtenbergstrasse 4, Garching, 85748, Germany.

[d] Shanghai Key Laboratory of Atmospheric Particle Pollution and Prevention (LAP3), Department of Environmental Science and Engineering, Fudan University, Shanghai 200438, China.

[e] Department of Civil and Environmental Engineering and Construction, University of Nevada, Las Vegas, NV 89154, USA.

[f] Department of Civil and Environmental Engineering, Imperial College London, South Kensington Campus, London SW7 2AZ, UK.

* Corresponding author email: dan.tsang@polyu.edu.hk

Abstract

Energy-saving, chemical-free, and high-efficiency microwave (MW)-assisted water treatment can be greatly facilitated *via* tailored design of an economical, sustainable, and 'green' carbonaceous catalyst. In this study, various biochars (BC) were pyrolyzed from two lignocellulosic waste biomasses, oak (O) and apple tree (A), at high temperature (900 °C) and under different gases (N_2 and CO_2). The holistic characterization by advanced spectroscopic techniques demonstrated that CO_2 pyrolysis of feedstock with more lignin (*i.e.*, oak), produced biochar with increased aromaticity and degree of carbonization. CO_2 modification created a hierarchical porous structure, improved surface hydrophilicity, polarity, and acidity, and provided higher

1

densities of near-surface functionalities of the biochar. Without MW irradiation, ABC-900C (1 g L^{-1}) provided the highest adsorption (52.6%, 1 min) of 2,4-dichlorophenoxy acetic acid (2,4-D) ascribed to large specific surface area, high micropore content, appropriate pore size, and abundant active groups. OBC-900C (1 g L^{-1}) enabled significantly increased 2,4-D removal (81.6%, 1 min) under MW irradiation (90 °C) in contrast with an oil bath (55.7%, 90 °C, 1 min) and room temperature (33.9%, 1 min) conditions, due to its highest graphitization degree and medium-developed microporous structure. The MW-induced thermal effect formed "hot spots" on the biochar surface as evidenced by elevated temperature of the bulk solution and lowered energy consumption of the MW reactor in the presence of OBC-900C, compared to those of the other biochars. The scavenging tests suggested that the generation of highly oxidative hydroxyl ($^{\bullet}$OH), anionic superoxide ($O_2^{\bullet-}$), and singlet oxygen ($^1O_2$) radicals contributed to the removal of 2,4-D. This study has demonstrated that biochar with customized structure and high organic adsorption capacity can act as an effective MW absorber suitable for rapid and improved removal of toxic organics.

Keywords: Microwave irradiation; Engineered biochar; Graphitic carbon; Sustainable waste management; Advanced wastewater treatment.

1. Introduction

With the rapid economic development, continuous industrialization, and increasing expectations of quality of life, large volumes of diverse chemicals have been discharging into aquatic ecosystems and causing severe water pollution [1]. Conventional wastewater treatment has become less efficient, and even advanced oxidation processes (AOPs) exhibit limitations including high demand of energy and need for additional chemicals, incomplete removal of refractory organic pollutants, and generation of more toxic intermediates derived from their parent compounds [2]. In recent years, microwave (MW)-assisted water treatment has emerged as a promising technology [3,4]. MW irradiation, which has a wide range of frequency (0.3–300

GHz) and wavelength (1–0.001 m) [3], provides selective, volumetric, uniform, and non-contact heating for MW-absorbing materials (*i.e.*, MW catalysts) [4,5], and induces rapid and non-gradient temperature ramping. The thermal effect of MW irradiation may produce "hot spots" or micro-plasmas that ionize the surrounding atmosphere [6], which can accelerate organic decomposition and generate highly oxidative hydroxyl radicals ($^{\bullet}$OH) [4,6]. MW irradiation treatment presents advantages compared to other heating techniques of easy operation, improved processing efficiency, reduced energy and chemical consumption, shortened reaction time, and complete mineralization of organic contaminants [3,7].

MW catalysts usually consist of a single (or binary/ternary) metallic phase (*e.g.*, Fe [8], Cu [9], Mn [10], Ni [11], Ti [12], Co [13], and Bi [14]), supported on porous, conductive materials (*e.g.*, activated carbon (AC) [15], mesoporous carbon [16], reduced graphene oxide (rGO) [17], and minerals [18]), which favour dispersion of metals/metal oxides and accelerate recycling of metal redox pairs [17]. Nonetheless, these catalysts are prone to deactivation *via* metal leaching/detachment creating a new environmental problem [6]. In contrast, metal-free carbon materials display strong thermal stability and robust anti-oxidation abilities that maintain good catalytic performance upon repeated use [4]. Carbonaceous materials with high dielectric loss tangent values (tan δ) are powerful MW absorbers [16], but seldom explored so far as MW catalysts for organics removal. Zhang et al. reported a MW-induced complete (97.9%) degradation of congo red (50 mg L^{-1}, 25 mL) catalyzed by commercial granular AC powder (2.0 g L^{-1}) in 2.5 min; however, no direct evidence was provided for the generation of reactive oxidative species (ROSs) and "hot spots" [20]. Veksha et al. claimed that MW irradiation on woodchip-derived AC (600 °C pyrolysis for 30 min followed by 10-min CO_2 activation at 780 °C) could not initiate the formation of "hot spots" or radicals for methyl orange (MO) decomposition [21]. Chen et al. reported MW-enhanced removal (100% within 7 min) of MO (25 mg L^{-1}, 25 mL) due to the formation of $^{\bullet}$OH over commercial multi-walled carbon nanotubes (CNTs) [22], yet did not discuss the existence of "hot spots" and differentiate organic adsorption from degradation [22]. In addition to

3

a lack of conclusive findings or solid evidence of MW-directed organic removal, the reported materials (AC and CNTs) were produced or purchased without science-informed design for high-performance functionalities under MW irradiation. Thus, there is a need for tailoring economical, sustainable, and 'green' carbon catalysts with favourable physicochemical characteristics, to achieve efficient MW absorption and fast removal of refractory organic pollutants.

Biochar is a carbon-rich solid material with aromatic surfaces produced *via* cost-effective thermal decomposition of various biomasses [23,24], including lignocellulosic wastes or residues from agricultural and forestry activities as the renewable feedstocks, under inert conditions [23,25]. Biochar finds wide applications in soil remediation [26,27], carbon dioxide (CO_2) sequestration [28,29], decontamination of heavy metals [30,31], degradation of organic pollutants [32,33], biorefinery [34,35], and energy storage [36]. Its outstanding performance is attributed to the hierarchical porous structure and abundant surface functionalities, which are primarily dependent on the synthesis conditions including biomass composition (*e.g.*, cellulose, hemicellulose, and lignin), pyrolysis temperature, and atmosphere (*e.g.*, N_2 and CO_2) [37]. Our recent studies revealed that high-temperature pyrolysis and CO_2 modification induced carbon reforming to improve the porous structure, increase carbonization level, and facilitate interface chemical interaction of biochar [38,39]. Herein, we hypothesize that: (i) MW-assisted organic compound removal is a combined process of simultaneous adsorption and degradation by biochar; (ii) highly porous and graphitic biochar with high MW absorption and organic adsorption capacities could act as effective MW-catalysts; and (iii) enhanced organic sequestration under MW irradiation catalyzed by biochar is attributed to the MW-induced thermal effect on the biochar surface.

In this study, two common lignocellulosic biomasses, oak tree (22 *wt.%* cellulose, 23 *wt.%* hemicellulose, and 55 *wt.%* lignin) and apple tree (43 *wt.%* cellulose, 22 *wt.%* hemicellulose, and 35 *wt.%* lignin) [23], with trace amounts of transition metals were selected as biochar feedstocks. Various biochars were prepared under

4

a high temperature (900 °C) and different purging gases (N_2 and CO_2). The easily mobilized 2,4-dichlorophenoxy acetic acid (2,4-D) was selected as a target refractory organic contaminant, as it has a high water solubility (900 mg L^{-1}), anionic nature (pK_a = 2.7), recalcitrant chemical structure, and low biodegradability, and is one of the most widely used herbicides and possible human carcinogens with moderate toxicity [40]. The objectives of this study were to: (i) articulate the interactions of several pyrolysis parameters (*i.e.*, feedstock type and gaseous medium) for tailoring the biochar physicochemical properties, surface structure, and interfacial chemical behaviour; and (ii) capitalize on the evolution of MW-induced thermal effect for biochar-catalyzed organic removal *via* generation of "hot spots" and various ROSs. The results of this study are conducive to improving the future design of high-efficiency, sustainable, and 'green' engineered carbon catalysts for application of MW irradiation in wastewater treatment.

2. Materials and methods

2.1. Biomass and chemicals

Waste wood biomasses of oak tree and apple tree were collected from Wuxi city (Jiangsu province, China) and Guiyang city (Guizhou province, China), respectively, and were applied as biochar feedstocks without further treatment. All chemicals used in this study (*viz.* 2,4-dichlorophenoxyacetic acid ($C_8H_6Cl_2O_3$, 2,4-D), *tert*-butanol ($C_4H_{10}O$, TBA), chloroform ($CHCl_3$, CF), furfuryl alcohol ($C_5H_6O_2$, FFA), methanol (CH_3OH), ethanol (C_2H_5OH), hexane (C_6H_{14}), acetonitrile (CH_3CN), dimethylsulfoxide ($(CH_3)_2SO$, DMSO), and acetic acid (CH_3COOH)) were of analytical reagent grade and solvents were of high-performance liquid chromatography (HPLC) grade from Sigma-Aldrich Co. Lit. (St. Louis, USA). Ultrapure water (UW, 18.2 MΩ cm), obtained from a Millipore Milli-Q Water Purification System (Milford, USA), was employed for all experimental aqueous solutions.

2.2. Preparation of the biochars

Wood waste (oak tree and apple tree) were cut into small pieces (< 1 cm), crushed and sieved through a 120-mesh (particle size < 0.125 mm), and then pyrolyzed in a tube furnace that was heated to 900 °C at a heating rate of 10 °C min^{-1}, and lasted for 2 h after reaching the target temperature with continuous N_2 or CO_2 purging at a flow rate of 200 mL min^{-1}. After being cooled down to room temperature (23 ±2 °C) inside the furnace, the samples were taken out, ground and passed through a 200-mesh sieve (particle size < 0.075 mm), and stored in airtight containers before use. The obtained oak and apple tree biochars were denoted as OBC-900N, OBC-900C, ABC-900N, and ABC-900C, respectively, where N/C corresponded to N_2/CO_2 purging.

2.3. Characterization of the biochars

The ultimate elemental analysis (EA, Vario EL cube, Germany) was used to estimate the CHONS elemental ratio in the biochar samples. The surface morphology and approximate surface elemental analysis of the obtained biochar samples were observed using scanning electron microscopy coupled with energy-dispersive X-ray spectroscopy (SEM-EDS, JSM-IT300, JXA-8230, Hitachi, Japan). The textural characteristics were determined using N_2 adsorption-desorption isotherms obtained from a surface area analyzer (Quantachrome Autosorb, USA) at 77 K for Brunauer-Emmett-Teller (BET) surface area and Barrett-Joyner-Halenda (BJH) porosity analyses. The Fourier transform infrared (FTIR, Nicolet 6700 spectrometer, USA) spectroscopy was used to observe the near-surface functionalities on biochars with the wavelength range at 400–4000 cm^{-1}. The micro-Raman spectrometer (Raman spectra, Renishwa Invia Fellex, UK) equipped with a Diode-Pumped Solid State (DPSS) at 532 nm excitation was used to record the defective level and graphitization degree of the biochars. The X-ray photoelectron spectroscopy (XPS, Thermo Fisher Scientific, USA) with Al Kα radiation was used to investigate the composition and chemical state of the elements on the sample surfaces. The binding energy of all characteristic peaks were calibrated with carbon C1s core level at 284.8 eV. Devolution of XPS data was conducted using Shirley background associated with Gaussian-Lorentzian model in XPSPEAK41, and the component peaks were identified by comparison of

6

their binding energies (BEs) with the reported values in the literature.

2.4. MW-assisted removal of 2,4-D by the biochars

The 2,4-D solution was prepared at an initial concentration of 100 mg L^{-1} (in accordance with the average concentration reported in 2,4-D manufacturing wastewaters [41,42]) by dissolving a certain amount of $C_8H_6Cl_2O_3$ in 1 L UW under magnetic stirring at 200 rpm for 6 h. To initiate the reaction, 20 mL of the 2,4-D solution and 20 mg of the biochars (OBC-900N, OBC-900C, ABC-900N, and ABC-900C, respectively) were added in 100 mL Teflon reaction vessels without pH adjustment and heated in the Ethos UP MW Reactor (Milestone, 2450 MHz, maximum power of 1900 W) under continuous magnetic stirring. The biochar loading (*i.e.*, 1 g L^{-1}) was determined according to preliminary experiments (data not shown) for obtaining relatively high 2,4-D removal by the four biochars with distinguishable differences. The MW temperature was ramped from room temperature to 90 °C within 2 min, held for 1 min, and gradually cooled down to below 60 °C by continuous mechanical ventilation in the MW reactor. The adopted reaction temperature and duration were comparable to previous studies on MW-assisted organic removal [20-22]. After reaction, an aliquot of 1 mL solution was withdrawn from the vessels, filtered into HPLC sample vials through 0.45 μm pore-size mixed cellulose ester membrane filters (MCE, Millipore), and tested for 2,4-D concentration by HPLC. The spent biochars were recovered by vacuum filtration, rinsed with UW, and oven dried at 60 °C overnight. The reusability of biochars was investigated by reacting spent samples (1 g L^{-1}) with 20 mL solution of 2,4-D (100 mg L^{-1}) in the MW reactor. A control experiment with only MW and no biochar was conducted. A comparative experiment using oil bath as the heating source was also performed under the same reaction conditions. The adsorption of 2,4-D by biochars was investigated at room temperature. No leaching of metals, organics, or nutrients was detected from the four biochars under the studied experimental conditions.

To verify the *in-situ* formation of radicals, such as •OH, anionic superoxide radical ($O_2^{•-}$), and singlet oxygen ($^1O_2$), during MW-assisted removal of 2,4-D, certain quantities of different organic scavengers (TBA

7

(k_{OH} = (3.2–7.6) × 10^8 M^{-1} s^{-1}), CF ($k_{O_2^-}$ = (1.1–3.2) × 10^9 M^{-1} s^{-1}), and FFA ($k_{^1O_2}$ = 1.2 × 10^8 M^{-1} s^{-1}),

respectively) were doped into the MW vessels to reach the target concentration of 45.2 mmol (at molar ratio

to 2,4-D of 100:1) [39,43], respectively. The radical quenching experiment was conducted under the same

MW/oil bath/room temperature conditions.

To extract adsorbed 2,4-D and possible degradation intermediates, after 1-min reaction in the three systems,

the spent samples were: (i) transferred into 20 mL solution of organic solvent (methanol, ethanol, hexane,

acetonitrile, and DMSO, respectively) under 8-h end-over-end shaking at 30 rpm [40]; or (ii) added into 20

mL mixed solution of water and different organic solvents (50%, *v/v*) under 1-min reaction in MW reactors

at 90 °C [21]. The above solutions were then analyzed for the extracted 2,4-D.

2.5. Analytical methods

The samples were analyzed for 2,4-D by a HPLC (Hitachi Chromaster 5420, Japan, limit of detection

(LOD) of 0.1 mg L^{-1}) equipped with an ODS-2 chromatography column (150 mm × 4.6 mm, 5 μm) and an

ultraviolet and visible spectrophotometry (UV-VIS) detector with UV wavelength set at 280 nm [44]. A

mixture of 60% (*v/v %*) acetonitrile, 38% (*v/v %*) UW, and 2% (*v/v %*) acetic acid was used as the mobile

phase at a flow rate of 0.5 mL min^{-1} [44]. The peak for 2,4-D was detected at a retention time of 5.6 min [44].

The total organic carbon (TOC) concentration was measured by a TOC analyzer (Shimadzu, SSM-5000A,

Japan, LOD of 0.1 mg L^{-1}). The 2,4-D or TOC removal efficiency was calculated using **Eq. 1** as follows.

Removal efficiency = ($C_{initial}$ − C_{final}) / $C_{initial}$ × 100%   (**Eq.1**)

Standard calibration was carried out prior to each analysis. Standards were analyzed every 10 samples for

quality assurance and quality control. All experiments were performed in at least triplicate, and the results are

presented as mean ± standard deviations. One-way analysis of variance (ANOVA) by the Duncan test was

applied to analyze the significance of differences between data (SPSS version 22.0). The lower-case letters in

the figures represent data grouping based on the significance level of 0.05 ($p < 0.05$).

3. Results and discussion

3.1. Characterization of the biochars

The distinctive physicochemical properties of the various biochars prepared from different feedstocks under N_2/CO_2 purging are summarized in **Table 1**. Pyrolysis of the lignin-rich biomass (*i.e.,* oak wood) produced biochars (OBC-900N and OBC-900C) with higher yield (20.8 and 19.8%) and carbon content (92.1 and 88.6 *wt.%*). Switching the purging gas from N_2 to CO_2 noticeably lowered the yield (from 19.8 to 17.0%) and carbon content (from 88.8 to 78.9 *wt.%*) of the resultant ABC-900s. These indicated that thermal decomposition of biomass in a CO_2 environment is more significant than that in a N_2 atmosphere, probably due to accelerated consumption of carbon matrix by CO_2 and other active gases produced during pyrolysis [45,46]. The elemental analysis revealed that the OBC-900s exhibited much lower molar ratios of H/C (0.010 of the OBC-900C and 0.011 of the OBC-900N) than the ABC-900s (0.025 of the ABC-900C and 0.079 of the ABC-900N), suggesting an increased biochar aromaticity with higher lignin content in the feedstocks and using CO_2 pyrolysis. The higher molar ratio of (O+N)/C of the ABC-900C (0.200) compared to ABC-900N (0.096) indicated an improved hydrophilicity and polarity in CO_2. In particular, the ABC-900C contained a much higher oxygen content (20.3 *wt.%*) than the other three biochars, probably because of CO_2 induced carbon oxidation during cooling inside the tube furnace after pyrolysis [47]. The zeta potential of the OBC-900s was negative (-18.8 – -12.6 mV) in contrast to the positively charged surfaces of the ABC-900s (2.64 – 6.73 mV), which can be ascribed to the higher metal (*i.e.*, Ca, K, Mg, Na, Fe, and Al) content in the former (**Table 1**). The pH values of the CO_2 pyrolyzed biochars (10.8–10.9) were lower than those of the N_2 pyrolyzed biochars (11.2–12.4), despite their similar ash contents (**Table 1**). CO_2 may have acidified the biochars *via* the creation of more near-surface oxygen-containing functionalities [45,48], which could be verified by the XPS analysis in the subsequent discussion.

9

The SEM images clearly depict the morphological and structural differences in the biochars dependent on different feedstocks and purging gases (**Fig. 1**). The OBC-900s presented rougher surfaces because of their higher ash content (**Table 1**), while the ABC-900s exhibited more porous structures due to the hierarchical spatial structure of softwood (*e.g.*, apple tree) [23]. As shown in **Fig. 1**, micro- and meso-pores were highly developed inside the carbon matrix of the CO_2 biochars (*i.e.*, OBC-900C and ABC-900C). These were also evidenced by the surface area and pore size distribution of the biochars in **Table 1**. The BET surface area (S_{BET}, 479.9 or 510.5 $m^2\,g^{-1}$) and total pore volume (V_{total}, 0.325 or 0.349 $cm^3\,g^{-1}$) of biochars fabricated in a CO_2 environment (OBC-900C or ABC-900C) were significantly higher than those generated in a N_2 environment. The CO_2 medium promoted the formation of micropores (377.5 or 384.4 $m^2\,g^{-1}$) of the OBC-900C (or ABC-900C). The micropore volume also increased from 0.164 (ABC-900N, 46.8% of V_{total}) to 0.235 (ABC-900C, 67.4% of V_{total}) $cm^3\,g^{-1}$. The average pore diameter (D_p) increased from 2.53 nm for the OBC-900N to 2.90 nm for the OBC-900C, indicating that CO_2 acted as a pore-enlarging agent. Tar and volatile organics generated from an incomplete thermal degradation of lignin could block the pores in biochars [49]. Such pore blocking was suppressed in CO_2, which could expedit tar cracking/reforming *via* the thermo-dynamically favourable Boudouard reaction between the CO_2 and lignin-C (*viz.* $C + CO_2 \rightarrow CO$) at $\geq 720\ °C$ [50], resulting in highly porous biochars [45].

The near-surface chemical functionalities of the biochars were characterized by FTIR analysis, as shown in **Fig. 2**. The small peak at ~3760 cm^{-1} ascribed to the –OH group was present in the spectra of all the biochars except the ABC-900N [51]. The peaks between 1360 and 1450 cm^{-1} are due to the aromatic C=C rings [52,53], whereas the aromatic C–C rings appeared at ~760 cm^{-1} [54]. The high-temperature (900 °C) pyrolysis eliminated the O-containing functional groups from the biochar surface and increased the content of condensed aromatic rings [38,39] as a result of intensive decomposition of the aliphatic and phenolic organic compounds *via* dehydration of cellulosic and ligneous components [39]. Biomass with higher lignin

content in a CO_2 atmosphere can provide biochars with a higher level of carbonization, as evidenced by the increasing intensity of aromatic peaks in the order of ABC-900N < ABC-900C < OBC-900N < OBC-900C (**Fig. 2**), in accordance with the elemental analysis (**Table 1**).

The graphitization degree of the biochars was further investigated by Raman analysis (**Fig. 3**). The Raman spectra of the biochar samples were deconvoluted into five characteristics peaks that were assigned to sp^2 C–H of aromatic rings (S^1) at 1060 cm^{-1}, defect bands and small ordered fused benzene rings (D) at 1310 cm^{-1}, methyl group and amorphous carbon (V^1) at 1380 cm^{-1}, aromatics with 3–5 rings (G^1) at 1540 cm^{-1}, and highly ordered sp^2 graphitic carbon (G) at 1590 cm^{-1}, respectively [39]. The area ratio of the D peak to the G peak (A_D/A_G) of the CO_2 pyrolyzed composites (1.94–2.56) was smaller than that produced in N_2 (2.26–3.52), suggesting that a CO_2 medium induced higher aromaticity and graphitization within the carbon matrix during pyrolysis [45,50]. Higher proportions of the G (11.5–13.0%) and G^1 (2.58–6.72%) bands were formed in the OBC-900s. The ratio of A_D/A_G decreased when there was a larger lignin content in the feedstocks. The cellulose and hemicellulose with branched polymer structure and short side chains form volatile products during pyrolysis of wood biomass, whereas the lignin with complex crosslinking phenolic polymer structure contributes mainly to the biochar production [23]. At pyrolysis temperatures higher than 700 °C, the fragmentation and repolymerization of lignin monomers favour the biochar formation, which could be accelerated in the presence of CO_2 [23]. Thus, the CO_2 enhanced aromaticity could be attributed to accelerated conversion of lignin monomers [44].

XPS analysis was conducted to investigate the transformation of near-surface functional groups in various biochars (**Fig. 4**). For all the samples, the C 1s spectra consisted of three distinctive peaks that were attributed to the presence of aromatic C–C/C=C at 284.8 eV, C–O at 285.8 eV, and π–π* transition in aromatic rings at 288.3 eV, respectively [38]. As shown in **Fig. 4**, the ratio of aromatic C–C/C=C increased from 65.4–66.9%, for ABC-900s to 68.4–68.7% for OBC-900s. This observation reaffirmed the idea of an enhanced conversion

11

of the crosslinking C structure to condensed aromatic nature of biochars derived from lignin-rich feedstocks [23,39], agreeing with the elemental composition (**Table 1**), FTIR spectra (**Fig. 2**), and Raman spectra (**Fig. 3**). Moreover, by means of XPS analysis, oxygen-containing functional groups (C–O) were identifiable on the biochar surface, the ratio of which increased from 16.1% (ABC-900N) to 17.5% (ABC-900C) after CO_2 activation. This contradictory observation compared with FTIR analysis (**Fig. 2**) might be due to the effect of solution pH and pKa of biochar on the sensitivity of FTIR, which is a bulk technique that reflects the average bonding environment. The C–O might result from the interaction of CO_2 with organic/inorganic compounds in the biochar [49]. Moreover, the density of π–π* transition in aromatic rings increased from 14.7–15.1% in the OBC-900s to 17.0–17.1% in the ABC-900s (**Fig. 4**). According to a previous study [55], these functionalities (C–O and π–π* transition) on biochar could contribute to effective adsorption of 2,4-D. However, it should be acknowledged that the above discussion was mainly based on the peak fitting of XPS spectra, which might be complicated by the small differences between different biochars. More accurate analysis using advanced and computational techniques should also be pursued in future studies.

3.2. MW-assisted removal of 2,4-D by the biochars

Removal efficiencies of 2,4-D by various biochars under three reaction conditions (*i.e.*, room temperature, oil bath, and MW irradiation) are presented and compared in **Fig. 5**. CO_2 activated biochars (ABC-900C and OBC-900C) with increased S_{BET} (479.9 and 510.5 m^2 g^{-1}) and D_p (2.90 and 2.99 nm) gave better 2,4-D adsorption performance than the N_2-produced biochars. CO_2 modification significantly promoted 2,4-D adsorption on OBC-900 and ABC-900, with the equilibrium removal efficiency improved from 40.9 ±0.7 to 49.4 ±7.3% and from 41.8 ±1.5 to 69.8 ±7.0% (**Fig. S1 (Supporting Information**)) after 30-min reaction, respectively, at room temperature without heating. A previous study also discovered a positive correlation between the specific surface area of biochar (400–600 m^2 g^{-1}) and its 2,4-D adsorption capacity [40],

12

indicating that the progressive widening of micropores into mesopores accommodated more 2,4-D molecules with polar surface area of 47 Å^2 [40]. Apart from a porous structure, other physicochemical properties of biochar also determined its capacity for 2,4-D adsorption. Our study suggested ABC-900C as the best-performing adsorbent of 2,4-D at room temperature. It had a zeta potential of 2.64 mV **(Table 1)** and thus a positively charged surface that favoured electrostatic interaction with the anionic form of 2,4-D at solution pH > 2.7 [55]. In addition, biochars with higher content of the π–π* transition (17.1% of the ABC-900C, **Fig. 4**) as electron acceptor could strengthen attraction with the electron-rich benzene ring of 2,4-D as electron donor *via* π–π interaction [55]. Moreover, the abundant oxygen-containing functional groups (17.5% C–O, **Fig. 4**) in the ABC-900C could contribute more active sites for 2,4-D adsorption [55]. Thus, adsorption of 2,4-D by biochar was likely a result of electrostatic interaction, electron conjugation, and chemisorption [55].

The significantly promoted removal of 2,4-D under MW irradiation is clearly illustrated in **Fig. 5**. After 1-min reaction in the MW reactor, 2,4-D removal by the OBC-900C and OBC-900N was obviously increased to 81.6 ±0.8 and 57.4 ±4.1%, respectively, *i.e.*, ~2.3 times the removal efficiency under room temperature. No 2.4-D removal was observed under MW irradiation only in the absence of biochar due to the low volatility of 2,4-D. However, gas emission could be a potential problem of the MW system for semi-volatile and volatile contaminants. MW treatment outperformed conventional heating in an oil bath at the same reaction temperature (90 °C) for 1–30 min (**Fig. 5** and **Fig. S1**). In particular, the OBC-900C, which achieved the highest removal in MW, consumed less energy than the rest of the biochars during the temperature ramping (1.39 *vs.* 1.68 kW) and holding (0.275 *vs.* 0.601 kW) stages, despite the same heating programme (**Fig. 6**). This suggested a more efficient MW-to-thermal energy transformation over the MW-absorbing OBC-900C. Furthermore, its temperature profile showed overshooting (~1 °C) after the ramping, which was absent from the other biochars. The strong MW absorptivity of the OBC-900C might have induced localized overheating, which promoted the removal of 2,4-D. Thus, the OBC-900C could absorb maximal electromagnetic energy

that ultimately penetrates into its carbon matrix and quickly dissipate as heat or other forms of energy [4].

There was only a slight improvement of 2,4-D removal in the presence of the ABC-900C under MW irradiation (69.9 ±1.7%) compared to oil bath heating (62.4 ±0.6%), both of which were better than room-temperature treatment (52.6 ±4.2%) (**Fig. 5**). In addition, the OBC-750C (pyrolyzed at a lower temperature of 750 °C) exhibited a significantly inferior performance for 2,4-D removal under the three different reaction conditions (**Fig. 5**). These results indicate that biochar prepared from various feedstocks, purging gases, and pyrolysis temperatures exhibited a distinctive sensitivity to MW irradiation. Carbon materials have been explored as MW adsorbents due to their high dielectric loss that is usually dependent on two critical factors, the bonding state of carbon atoms (*i.e.*, degree of graphitization) and the microstructure of the carbon matrix [16]. On one hand, the large surface area ($S_{BET} = 510.5$ m^2 g^{-1}), high proportion of micropores ($V_{micro}/V_{total} = 67.4\%$), appropriate pore size ($D_p = 2.99$ nm), and abundant surface functionalities (17.5% C–O and 17.1% π–π* transition in aromatic rings) of the ABC-900C could guarantee sufficient adsorption of aquatic organic pollutants (**Table 1** and **Fig. 4**). On the other hand, the higher degree of graphitization of the OBC-900C ($A_D/A_G = 1.94$ and 68.7% aromatic C–C/C=C, **Figs. 3-4**), together with its greater microwave absorbing property and medium-developed microporous structure, would be beneficial to the capture and degradation of 2,4-D under MW irradiation.

The MW-enhanced organic removal may also be attributed to the formation of various ROSs catalyzed by the carbon surface [21]. As shown in **Fig. 7**, TBA addition only slightly decreased the 2,4-D removal to 34.2 ±0.8% by the ABC-900N while performances of the other biochars remained unaffected. In contrast, CF or FFA noticeably inhibited the 2,4-D removal to the same extent in the MW systems containing the OBC-900C and ABC-900C (44.5 ±5.6 − 52.8 ±0.7% and 20.4 ±0.4 − 22.3 ±4.2%, respectively) compared with 81.6 ±0.8 and 61.9 ±1.7% removal with no scavengers (**Fig. 7**), indicating the equal contribution of $O_2^{\bullet-}$ and $^1O_2$ to 2,4-D removal. However, in the case of N$_2$ pyrolyzed biochars , FFA led to a more significant decrease in 2,4-D

14

removal compared with CF, *i.e.,* 49.1 ±4.9 *vs.* 36.6 ±0.3% and 10.5 ±2.6 *vs.*3.1 ±0.8% for the OBC-900N and ABC-900N, respectively (**Fig. 7**), suggesting that $^1O_2$ played a superior role than the other ROSs. In particular, the additional organic scavengers did not exhibit noticeable effect on 2,4-D removal under room temperature or oil bath conditions. This observation excluded the potential interference of these organic scavengers on 2,4-D adsorption, and reaffirmed that radicals were only generated in the MW system. The production of radical species is summarized in reactions **R1**–**R3** according to previous studies [23]. Upon MW irradiation, water (H_2O) molecules surrounding biochar surface "hot spots" could be activated into $^•OH$ and hydrogen radicals ($^•H$) (**R1**). Oxygen (O_2) in the water medium would react with $^•H$ to form $O_2^{•-}$ and $^1O_2$ (**R2**), which could further yield $^•OH$ *via* **R3**. These radicals ($O_2^{•-}$ and $^1O_2$) with powerful oxidization capacity could decompose the adsorbed or soluble 2,4-D into intermediates with lower molecular weight, and finally mineralize into CO_2 and H_2O.

$$H_2O \xrightarrow{MW} {^•OH} + {^•H} \tag{R1}$$

$$2O_2 + {^•H} \xrightarrow{MW} {^1O_2} + O_2^{•-} + H^+ \tag{R2}$$

$$O_2^{•-} + 2H_2O \xrightarrow{MW} 3^•OH + OH^- \tag{R3}$$

3.3. Desorption and reusability of the biochars

To further distinguish adsorption and degradation of 2,4-D under the three reaction conditions (MW irradiation, oil bath, and room temperature), the adsorbed 2,4-D on the spent biochars were extracted by different organic solvents (methanol, ethanol, hexane, acetonitrile, and DMSO respectively) *via* desorption at room temperature and under MW conditions, respectively. However, neither desorption procedures with any organic solvent could recover more than 10% 2,4-D from the reacted samples. These results might be due to strong binding between 2,4-D and biochar *via* diffusion into the inner porous structure and intensive chemisorption by the surface functionalities of biochar [40]. In addition, the 1-min TOC removal (59.2 ±2.5,

15

43.3 ±0.9, 83.0 ±3.4, and 71.9 ±3.2%, respectively) by the OBC-900N, ABC-900N, OBC-900C, and ABC-900N, respectively, was slightly greater than the 2,4-D removal (57.4 ±4.1, 41.2 ±2.2, 81.6 ±0.8, and 69.9 ±1.7%, respectively) under MW conditions (**Fig. S2**). These results indicated that 2,4-D could be completely mineralized into CO_2 and H_2O by the MW-assisted removal in presence of biochar. Moreover, no obvious peaks of any degradation intermediates were observed by HPLC analysis of the solutions after reaction or the extraction solutions of the spent biochars, probably because of a strong entrapment of possible by-products by the biochars. Thus, no direct evidence of 2,4-D decomposition (within the accuracies of the experimental methods) could be provided in the current stage of our study. According to the latest findings [56], the dechlorination rate of 2,4-D (*i.e.*, change of the Cl^- concentration) was correlated to its degradation efficiency when 2,4-D was completely mineralized into CO_2 and H_2O. More comprehensive experimental design (*e.g.*, extraction of reacted biochars by other means, full identification of 2,4-D intermediates, and detection of released Cl^-) would help to further prove and quantify the 2,4-D degradation in the MW/biochar system.

Reusability of the OBC-900N and OBC-900C biochars was tested in three consecutive cycles of 2,4-D removal under MW irradiation. A progressive loss of biochar activity in each cycle is depicted in **Fig. 8**. Without any treatment of regeneration, the performance of the OBC-900C (or OBC-900N) noticeably dropped from 81.7 ±2.1% (or 61.2 ±0.9%) to 24.2 ±1.3% (or 21.2 ±1.1%) 2,4-D removal. This observation could be ascribed to the high BET surface area and internal microporous structure of biochar. The degradation by-products might accumulate and occupy the active sites on biochar surface for 2,4-D adsorption. It is also possible that the carbon materials eventually crumble when "hot spots" formed inside micropores generate sufficient confined vapour with increased pressure [6]. This so-called "popcorn effect" could impede biochar stability with susceptible deactivation and fouling by intermediates [6]. Future studies should focus on biochar regeneration *via* facile and low-cost treatment, for example, low-temperature heating in N_2 environment or desorption by various types of green solvents.

For future design of more sustainable water/wastewater treatment processes, MW technology can be effectively incorporated with membrane bioreactors and electro-/photo-catalysis process [3,4]. However, most current studies on MW system for water/wastewater treatment are conducted in laboratory scale, because (i) volume and power output of the available MW reactors are insufficient for widespread commercial promotion, and (ii) low-cost, highly efficient, and recyclable catalysts are critical for industrial applications [3,4]. With further development of equipment optimization and catalysts exploitation, MW technology is expected to deliver good benefits for practical water and wastewater treatment.

Conclusions

This study has demonstrated that biochar derived from waste biomass of oak tree, with high lignin content under 900 °C pyrolysis and CO_2 purging, can act as a 'green', highly efficient MW absorber. The CO_2 purging can promote decomposition of lignin carbon at high pyrolysis temperature *via* fragmentation and repolymerization, producing biochar with a developed hierarchical porous structure, enhanced graphitization level, and improved surface chemistry. Under mild MW irradiation, 2,4-D was simultaneously adsorbed (*via* electrostatic interaction, electron conjugation, and chemisorption) and degraded due to a MW-induced thermal effect on the biochar surface that generated hydroxyl ($^{\bullet}OH$), anionic superoxide ($O_2^{\bullet -}$), and singlet oxygen ($^1O_2$) radicals. This study has demonstrated the potential application of an economical, sustainable, metal-free biochar in energy-saving, chemical-free water/wastewater treatment using MW, which could make an important contribution to a clean water environment. Future studies are suggested to optimize the rational design of MW-active biochar catalysts and investigate the applicability of the MW/biochar system to a broader range of organic pollutants with diverse physicochemical properties in water/wastewater matrices.

Acknowledgement

References

[1] Sun, J., Pan, L., Tsang, D.C.W., Zhan, Y., Zhu, L., Li, X.D., Organic contamination and remediation in the agricultural soils of China: A critical review, Science of the Total Environment, 615 (2018), 724-740.

[2] Kümmerer, K., Dionysiou, D.D., Olsson, O., Fatta-Kassinos, D., A path to clean water. Science, 361 (2018), 222-224.

[3] Wei, R., Wang, P., Zhang, G., Wang, N., Zheng, T., Microwave-responsive catalysts for wastewater treatment: A review, Chemical Engineering Journal, (2020), 122781.

[4] Xue, C., Mao, Y., Wang, W., Song, Z., Zhao, X., Sun, J., Wang, Y., Current status of applying microwave-associated catalysis for the degradation of organics in aqueous phase-A review, Journal of Environmental Sciences, 81 (2019), 119-135.

[5] Varisli, D., Korkusuz, C., Dogu, T., Microwave-assisted ammonia decomposition reaction over iron incorporated mesoporous carbon catalysts., Applied catalysis B: Environmental, 201 (2017), 370-380.

[6] Garcia-Costa, A.L., Zazo, J.A., Rodriguez, J.J., Casas, J.A., Intensification of catalytic wet peroxide oxidation with microwave radiation: activity and stability of carbon materials, Separation and Purification Technology, 209 (2019), 301-306.

[7] Hu, L., Wang, P., Shen, T., Wang, Q., Wang, X., Xu, P., Zheng, Q., Zhang, G., The application of microwaves in sulfate radical-based advanced oxidation processes for environmental remediation: A review, Science of The Total Environment, (2020), 137831.

[8] Garcia-Costa, A.L., Zazo, J.A., Rodriguez, J.J., Casas, J.A., Microwave-assisted catalytic wet peroxide oxidation. Comparison of Fe catalysts supported on activated carbon and γ-alumina, Applied Catalysis B:

Environmental, 218 (2017), 637-642.

[9] Chen, J., Pan, H., Hou, H., Li, H., Yang, J., Wang, L., High efficient catalytic degradation of PNP over Cu-bearing catalysts with microwave irradiation, Chemical Engineering Journal, 323 (2017), 444-454.

[10] Wang, X., Mei, L., Xing, X., Liao, L., Lv, G., Li, Z., Wu, L., Mechanism and process of methylene blue degradation by manganese oxides under microwave irradiation, Applied Catalysis B: Environmental, 160 (2014), 211-216.

[11] Ahmed, A. B., Jibril, B., Danwittayakul, S., Dutta, J., Microwave-enhanced degradation of phenol over Ni-loaded ZnO nanorods catalyst, Applied Catalysis B: Environmental, 156 (2014), 456-465.

[12] Ling, L., Feng, Y., Li, H., Chen, Y., Wen, J., Zhu, J., Bian, Z., Microwave induced surface enhanced pollutant adsorption and photocatalytic degradation on Ag/TiO$_2$, Applied Surface Science, 483 (2019), 772-778.

[13] Qi, Y., Mei, Y., Li, J., Yao, T., Yang, Y., Jia, W., Tong, X., Wu, J., Xin, B., Highly efficient microwave-assisted Fenton degradation of metacycline using pine-needle-like CuCo$_2$O$_4$ nanocatalyst, Chemical Engineering Journal, 373 (2019), 1158-1167.

[14] Qiu, Y. and Zhou, J., Highly effective and green microwave catalytic oxidation degradation of nitrophenols over Bi$_2$O$_2$CO$_3$ based composites without extra chemical additives, Chemosphere, 214 (2019), 319-329.

[15] Yao, X., Lin, Q., Zeng, L., Xiang, J., Yin, G., & Liu, Q. (2017). Degradation of humic acid using hydrogen peroxide activated by CuO-Co$_3$O$_4$@ AC under microwave irradiation. Chemical Engineering Journal, 330, 783-791.

[16] Cai, B., Feng, J. F., Peng, Q. Y., Zhao, H. F., Miao, Y. C., Pan, H., Super-fast degradation of high concentration methyl orange over bifunctional catalyst Fe/Fe$_3$C@C with microwave irradiation, Journal of Hazardous Materials, 392 (2020), 122279.

[17] Yao, T., Qi, Y., Mei, Y., Yang, Y., Aleisa, R., Tong, X., Wu, J., One-step preparation of reduced graphene oxide aerogel loaded with mesoporous copper ferrite nanocubes: A highly efficient catalyst in microwave-assisted Fenton reaction, Journal of Hazardous mMaterials, 378 (2019), 120712.

[18] Shen, M., Fu, L., Tang, J., Liu, M., Song, Y., Tian, F., Zhao, Z., Zhang, Z., Dionysiou, D.D., Microwave hydrothermal-assisted preparation of novel spinel-$NiFe_2O_4$/natural mineral composites as microwave catalysts for degradation of aquatic organic pollutants, Journal of Hazardous Materials, 350 (2018), 1-9.

[20] Zhang, Z., Shan, Y., Wang, J., Ling, H., Zang, S., Gao, W., Zhao, Z., Zhang, H., Investigation on the rapid degradation of congo red catalyzed by activated carbon powder under microwave irradiation, Journal of Hazardous Materials, 147 (2007), 325-333.

[21] Veksha, A., Pandya, P., Hill, J.M., The removal of methyl orange from aqueous solution by biochar and activated carbon under microwave irradiation and in the presence of hydrogen peroxide, Journal of Environmental Chemical Engineering, 3 (2015), 1452-1458.

[22] Chen, J., Xue, S., Song, Y., Shen, M., Zhang, Z., Yuan, T., Tian, F., Dionysiou, D.D., Microwave-induced carbon nanotubes catalytic degradation of organic pollutants in aqueous solution, Journal of Hazardous Materials, 310 (2016), 226-234.

[23] Rangabhashiyam, S. and Balasubramanian, P., The potential of lignocellulosic biomass precursors for biochar production: performance, mechanism and wastewater application-A review, Industrial Crops and Products, 128 (2019), 405-423.

[24] Kumar, M., Xiong, X., Sun, Y., Iris, K.M., Tsang, D.C.W., Hou, D., Gupta, J., Bhaskard, T., Pandey, A., Critical review on biochar-supported catalysts for pollutant degradation and sustainable biorefinery. Advanced Sustainable Systems, (2020), 1900149.

[25] Shaheen, S.M., Niazi, N.K., Hassan, N.E., Bibi, I., Wang, H., Tsang, D.C.W., Ok., Y.S., Bolan, N., Rinklebe, J., Wood-based biochar for the removal of potentially toxic elements in water and wastewater:

a critical review, International Materials Reviews, 64 (2019), 216-247.

[26] El-Naggar, A., Lee, S.S., Awad, Y.M., Yang, X., Ryu, C., Rizwan, M., Rinklebe, J., Tsang, D.C.W., Ok, Y.S., Influence of soil properties and feedstocks on biochar potential for carbon mineralization and improvement of infertile soils, Geoderma, 332 (2018), 100-108.

[27] Igalavithana, A.D., Lee, S.E., Lee, Y.H., Tsang, D.C.W., Rinklebe, J., Kwon, E.E., Ok, Y.S., Heavy metal immobilization and microbial community abundance by vegetable waste and pine cone biochar of agricultural soils, Chemosphere, 174 (2017), 593-603.

[28] Dissanayake, P.D., Choi, S.W., Igalavithana, A.D., Yang, X., Tsang, D.C.W., Wang, C.H., Kua, H.W., Lee, K.B., Ok, Y.S., Sustainable gasification biochar as a high efficiency adsorbent for CO_2 capture: A facile method to designer biochar fabrication, Renewable and Sustainable Energy Reviews, 124 (2020), 109785.

[29] Xu, X., Xu, Z., Gao, B., Zhao, L., Zheng, Y., Huang, J., Tsang, D.C.W., Ok, Y.S., Cao, X., New insights into CO_2 sorption on biochar/Fe oxyhydroxide composites: Kinetics, mechanisms, and in situ characterization, Chemical Engineering Journal, 384 (2020), 123289.

[30] Sun, Y., Chen, S.S., Lau, A.Y.T., Tsang, D.C.W., Mohanty, S.K., Bhatnagar, A., Rinklebe, J., Lin, A.K.Y., Ok, Y.S. Waste-derived compost and biochar amendments for stormwater treatment in bioretention column: Co-transport of heavy metals and colloid, Journal of Hazardous Materials, 383 (2020), 121243.

[31] Rajapaksha, A.U., Alam, M.S., Chen, N., Alessi, D.S., Igalavithana, A.D., Tsang, D.C.W., Ok, Y.S., Removal of hexavalent chromium in aqueous solutions using biochars: Chemical and spectroscopic investigations. Science of the Total Environment, 625 (2018), 1567-1573.

[32] Ruan, X., Sun, Y., Du, W., Tang, Y., Liu, Q., Zhang, Z., William, D., Ray L.F., Qian, R., Tsang, D.C.W., Formation, characteristics, and application of environmentally persistent free radicals (EPFRs) in biochars and environmental matrices: A Review, Bioresource Technology, 281 (2019), 457-468.

[33] Li, Z., Sun, Y., Yang, Y., Han, Y., Wang, T., Chen, J., Tsang, D.C.W., Biochar-supported nanoscale zero-valent iron as an efficient catalyst for organic degradation in groundwater, Journal of Hazardous Materials, 383 (2020), 121240.

[34] Yu, I.K.M., Xiong, X., Tsang, D.C.W., Wang, L., Hunt, A.J., Song, H., Shang, J., Ok, Y.S., Poon, C.S., Aluminium-biochar composite as a sustainable heterogeneous catalyst for glucose isomerization in biorefinery, Green Chemistry, 21 (2019), 1267-1281.

[35] Xiong, X., Yu, I.K.M., Cao, L., Tsang, D.C.W., Zhang, S., Ok, Y.S., A review of biochar-based catalysts for chemical synthesis, biofuel production, and pollution control. Bioresource Technology, 246 (2017), 254-270.

[36] Mian, M.M., Liu, G., Fu, B., Conversion of sewage sludge into environmental catalyst and microbial fuel cell electrode material: A review, Science of The Total Environment, 666 (2019), 525-539.

[37] Sun, C., Chen, T., Huang, Q., Zhan, M., Li, X., Yan, J., Activation of persulfate by CO_2-activated biochar for improved phenolic pollutant degradation: Performance and mechanism, Chemical Engineering Journal, 380 (2020), 122519.

[38] Sun, Y., Yu, I.K.M., Tsang, D.C.W., Cao, X.D, Lin, D.H, Wang, L.L, Graham, N.J.D., Daniel, S.A., Michael, K., Ok, Y.S., Feng, Y.J., Li, X.D. Multifunctional iron-biochar composites for the removal of potentially toxic elements, inherent cations, and hetero-chloride from hydraulic fracturing wastewater, Environment International, 124 (2019), 521-532.

[39] Wan, Z., Sun, Y., Tsang, D.C.W., Yu, I.K.M., Fan, J., Clark, J.H., Zhou, Y., Cao, X., Gao, B., Ok, Y.S., Sustainable biochar catalyst synergized with copper heteroatoms and CO_2 for singlet oxygenation and electron transfer routes, Green Chemistry, 21 (2019), 4800.

[40] Mandal, S., Sarkar, B., Igalavithana, A.D., Ok, Y.S., Yang, X., Lombi, E., Bolan, N., Mechanistic insights of 2, 4-D sorption onto biochar: Influence of feedstock materials and biochar properties, Bioresource

Technology, 246 (2017), 160-167.

[41] Tiwari, B., Sellamuthu, B., Ouarda, Y., Drogui, P., Tyagi, R.D., Buelna, G., Review on fate and mechanism of removal of pharmaceutical pollutants from wastewater using biological approach, Bioresource Technology, 224 (2017), 1-12.

[42] Shi, X., Leong, K.Y., Ng, H.Y., Anaerobic treatment of pharmaceutical wastewater: a critical review. Bioresource Technology, 245 (2017), 1238-1244.

[43] Wang, D., Sun, Y., Tsang, D.C.W., Khan, E., Cho, D.W., Zhou, Y., Qi, F., Gong, J., Wang, L., Synergistic utilization of inherent halides and alcohols in hydraulic fracturing wastewater for radical-based treatment: A case study of di-(2-ethylhexyl) phthalate removal, Journal of Hazardous Materials, 384 (2020), 121321.

[44] Cho, D.W., Yoon, K., Ahn, Y., Sun, Y., Tsang, D.C.W., Hou, D., Ok, Y.S., Song, H., Fabrication and environmental applications of multifunctional mixed metal-biochar composites (MMBC) from red mud and lignin wastes, Journal of Hazardous Materials, 374 (2019), 412-419.

[45] Lee, J., Yang, X., Cho, S.H., Kim, J.K., Lee, S.S., Tsang, D.C.W., Ok, Y.S., Kwon, E.E., Pyrolysis process of agricultural waste using CO_2 for waste management, energy recovery, and biochar fabrication. Applied Energy, 185 (2017), 214-222.

[46] Qian, F., Zhu, X., Liu, Y., Hao, S., Ren, Z.J., Gao, B., Zong, R., Zhang, S., Chen, J., Synthesis, characterization and adsorption capacity of magnetic carbon composites activated by CO_2: implication for the catalytic mechanisms of iron salts, Journal of Materials Chemistry A, 4 (2016), 18942-18951.

[47] Yang, X., Yu, I.K.M., Cho, D.W., Chen, S.S., Tsang, D.C.W., Shang, J., Yip, A.C.K., Wang, L., Ok, Y.S., Tin-functionalized wood biochar as a sustainable solid catalyst for glucose isomerization in biorefinery, ACS Sustainable Chemistry & Engineering, 7 (2019), 4851-4860.

[48] Liu, Y., Zhu, X., Wei, X., Zhang, S., Chen, J., Ren, Z. J., CO_2 activation promotes available carbonate

and phosphorus of antibiotic mycelial fermentation residue-derived biochar support for increased lead immobilization, Chemical Engineering Journal, 334 (2018), 1101-1107.

[49] Igalavithana, A.D., Yang, X., Zahra, H.R., Tack, F.M., Tsang, D.C.W., Kwon, E.E., Ok, Y.S., Metal (loid) immobilization in soils with biochars pyrolyzed in N_2 and CO_2 environments, Science of the total environment, 630 (2018), 1103-1114.

[50] Kim, Y., Oh, J.I., Vithanage, M., Park, Y.K., Lee, J., Kwon, E.E., Modification of biochar properties using CO_2, Chemical Engineering Journal, 372 (2019), 383-389.

[51] Peng, Y., Sun, Y., Sun, R., Zhou, Y., Tsang, D.C.W., Chen, Q., Optimizing synthesis of Fe/Al (hydr)oxides-biochars to maximize phosphorus removal via response surface model, Journal of Cleaner Production, 237 (2019), 117770.

[52] Yang, F., Zhang, S., Sun, Y., Cheng, K., Li, J., Tsang, D.C.W., Fabrication and characterization of hydrophilic corn stalk biochar-supported nanoscale zero-valent iron composites for efficient metal removal, Bioresource Technology, 265 (2018), 490-497.

[53] Yang, F., Zhang, S., Sun, Y., Tsang, D.C.W., Cheng, K., Ok, Y.S., Assembling biochar with various layered double hydroxides for enhancement of phosphorus recovery, Journal of Hazardous Materials, 365 (2019), 665-673.

[54] Yang, F., Zhang, S., Sun, Y., Du. Q., Song J.P., Tsang, D.C.W., A novel electrochemical modification combined with one-step pyrolysis for preparation of sustainable thorn-like iron-based biochar composites, Bioresource Technology, 274 (2019), 379-385.

[55] Zhu, L., Zhao, N., Tong, L., Lv, Y., Li, G., Characterization and evaluation of surface modified materials based on porous biochar and its adsorption properties for 2, 4-dichlorophenoxyacetic acid, Chemosphere, 210 (2018), 734-744.

[56] Li, W., Li, Y., Zhang, D., Lan, Y., Guo, J., CuO-Co_3O_4@CeO_2 as a heterogeneous catalyst for efficient

degradation of 2, 4-dichlorophenoxyacetic acid by peroxymonosulfate, Journal of Hazardous Materials,

381 (2020), 121209.

Tailored design of graphitic biochar for high-efficiency and chemical-free microwave-assisted removal of refractory organic contaminants

Yuqing Sun [a], Iris K.M. Yu [b,c], Daniel C.W. Tsang [a,*], Jiajun Fan [b], James H. Clark [b,d], Gang Luo [d], Shicheng Zhang [d], Eakalak Khan [e], Nigel J.D. Graham [f]

[a] Department of Civil and Environmental Engineering, The Hong Kong Polytechnic University, Hung Hom, Kowloon, Hong Kong, China.

[b] Green Chemistry Centre of Excellence, Department of Chemistry, University of York, York, YO10 5DD, UK.

[c] Department of Chemistry and Catalysis Research Center, Technische Universität München, Lichtenbergstrasse 4, Garching, 85748, Germany.

[d] Shanghai Key Laboratory of Atmospheric Particle Pollution and Prevention (LAP3), Department of Environmental Science and Engineering, Fudan University, Shanghai 200438, China.

[e] Department of Civil and Environmental Engineering and Construction, University of Nevada, Las Vegas, NV 89154, USA.

[f] Department of Civil and Environmental Engineering, Imperial College London, South Kensington Campus, London SW7 2AZ, UK.

* Corresponding author email: dan.tsang@polyu.edu.hk

Abstract

Energy-saving, chemical-free, and high-efficiency microwave (MW)-assisted water treatment can be greatly facilitated *via* tailored design of an economical, sustainable, and 'green' carbonaceous catalyst. In this study, various biochars (BC) were pyrolyzed from two lignocellulosic waste biomasses, oak (O) and apple tree (A), at high temperature (900 °C) and under different gases (N_2 and CO_2). The holistic characterization by advanced spectroscopic techniques demonstrated that CO_2 pyrolysis of feedstock with more lignin (*i.e.*, oak), produced biochar with increased aromaticity and degree of carbonization. CO_2 modification created a hierarchical porous structure, improved surface hydrophilicity, polarity, and acidity, and provided higher

densities of near-surface functionalities of the biochar. Without MW irradiation, ABC-900C (1 g L^{-1}) provided the highest adsorption (52.6%, 1 min) of 2,4-dichlorophenoxy acetic acid (2,4-D) ascribed to large specific surface area, high micropore content, appropriate pore size, and abundant active groups. OBC-900C (1 g L^{-1}) enabled significantly increased 2,4-D removal (81.6%, 1 min) under MW irradiation (90 °C) in contrast with an oil bath (55.7%, 90 °C, 1 min) and room temperature (33.9%, 1 min) conditions, due to its highest graphitization degree and medium-developed microporous structure. The MW-induced thermal effect formed "hot spots" on the biochar surface as evidenced by elevated temperature of the bulk solution and lowered energy consumption of the MW reactor in the presence of OBC-900C, compared to those of the other biochars. The scavenging tests suggested that the generation of highly oxidative hydroxyl ($^{\bullet}$OH), anionic superoxide ($O_2^{\bullet-}$), and singlet oxygen ($^1O_2$) radicals contributed to the removal of 2,4-D. This study has demonstrated that biochar with customized structure and high organic adsorption capacity can act as an effective MW absorber suitable for rapid and improved removal of toxic organics.

Keywords: Microwave irradiation; Engineered biochar; Graphitic carbon; Sustainable waste management; Advanced wastewater treatment.

1. Introduction

With the rapid economic development, continuous industrialization, and increasing expectations of quality of life, large volumes of diverse chemicals have been discharging into aquatic ecosystems and causing severe water pollution [1]. Conventional wastewater treatment has become less efficient, and even advanced oxidation processes (AOPs) exhibit limitations including high demand of energy and need for additional chemicals, incomplete removal of refractory organic pollutants, and generation of more toxic intermediates derived from their parent compounds [2]. In recent years, microwave (MW)-assisted water treatment has emerged as a promising technology [3,4]. MW irradiation, which has a wide range of frequency (0.3–300

GHz) and wavelength (1–0.001 m) [3], provides selective, volumetric, uniform, and non-contact heating for MW-absorbing materials (*i.e.*, MW catalysts) [4,5], and induces rapid and non-gradient temperature ramping. The thermal effect of MW irradiation may produce "hot spots" or micro-plasmas that ionize the surrounding atmosphere [6], which can accelerate organic decomposition and generate highly oxidative hydroxyl radicals (•OH) [4,6]. MW irradiation treatment presents advantages compared to other heating techniques of easy operation, improved processing efficiency, reduced energy and chemical consumption, shortened reaction time, and complete mineralization of organic contaminants [3,7].

MW catalysts usually consist of a single (or binary/ternary) metallic phase (*e.g.*, Fe [8], Cu [9], Mn [10], Ni [11], Ti [12], Co [13], and Bi [14]), supported on porous, conductive materials (*e.g.*, activated carbon (AC) [15], mesoporous carbon [16], reduced graphene oxide (rGO) [17], and minerals [18]), which favour dispersion of metals/metal oxides and accelerate recycling of metal redox pairs [17]. Nonetheless, these catalysts are prone to deactivation *via* metal leaching/detachment creating a new environmental problem [6]. In contrast, metal-free carbon materials display strong thermal stability and robust anti-oxidation abilities that maintain good catalytic performance upon repeated use [4]. Carbonaceous materials with high dielectric loss tangent values (tan δ) are powerful MW absorbers [16], but seldom explored so far as MW catalysts for organics removal. Zhang et al. reported a MW-induced complete (97.9%) degradation of congo red (50 mg L^{-1}, 25 mL) catalyzed by commercial granular AC powder (2.0 g L^{-1}) in 2.5 min; however, no direct evidence was provided for the generation of reactive oxidative species (ROSs) and "hot spots" [20]. Veksha et al. claimed that MW irradiation on woodchip-derived AC (600 °C pyrolysis for 30 min followed by 10-min CO_2 activation at 780 °C) could not initiate the formation of "hot spots" or radicals for methyl orange (MO) decomposition [21]. Chen et al. reported MW-enhanced removal (100% within 7 min) of MO (25 mg L^{-1}, 25 mL) due to the formation of •OH over commercial multi-walled carbon nanotubes (CNTs) [22], yet did not discuss the existence of "hot spots" and differentiate organic adsorption from degradation [22]. In addition to

a lack of conclusive findings or solid evidence of MW-directed organic removal, the reported materials (AC and CNTs) were produced or purchased without science-informed design for high-performance functionalities under MW irradiation. Thus, there is a need for tailoring economical, sustainable, and 'green' carbon catalysts with favourable physicochemical characteristics, to achieve efficient MW absorption and fast removal of refractory organic pollutants.

Biochar is a carbon-rich solid material with aromatic surfaces produced *via* cost-effective thermal decomposition of various biomasses [23,24], including lignocellulosic wastes or residues from agricultural and forestry activities as the renewable feedstocks, under inert conditions [23,25]. Biochar finds wide applications in soil remediation [26,27], carbon dioxide (CO_2) sequestration [28,29], decontamination of heavy metals [30,31], degradation of organic pollutants [32,33], biorefinery [34,35], and energy storage [36]. Its outstanding performance is attributed to the hierarchical porous structure and abundant surface functionalities, which are primarily dependent on the synthesis conditions including biomass composition (*e.g.*, cellulose, hemicellulose, and lignin), pyrolysis temperature, and atmosphere (*e.g.*, N_2 and CO_2) [37]. Our recent studies revealed that high-temperature pyrolysis and CO_2 modification induced carbon reforming to improve the porous structure, increase carbonization level, and facilitate interface chemical interaction of biochar [38,39]. Herein, we hypothesize that: (i) MW-assisted organic compound removal is a combined process of simultaneous adsorption and degradation by biochar; (ii) highly porous and graphitic biochar with high MW absorption and organic adsorption capacities could act as effective MW-catalysts; and (iii) enhanced organic sequestration under MW irradiation catalyzed by biochar is attributed to the MW-induced thermal effect on the biochar surface.

In this study, two common lignocellulosic biomasses, oak tree (22 *wt.%* cellulose, 23 *wt.%* hemicellulose, and 55 *wt.%* lignin) and apple tree (43 *wt.%* cellulose, 22 *wt.%* hemicellulose, and 35 *wt.%* lignin) [23], with trace amounts of transition metals were selected as biochar feedstocks. Various biochars were prepared under

a high temperature (900 °C) and different purging gases (N_2 and CO_2). The easily mobilized 2,4-dichlorophenoxy acetic acid (2,4-D) was selected as a target refractory organic contaminant, as it has a high water solubility (900 mg L^{-1}), anionic nature ($pK_a = 2.7$), recalcitrant chemical structure, and low biodegradability, and is one of the most widely used herbicides and possible human carcinogens with moderate toxicity [40]. The objectives of this study were to: (i) articulate the interactions of several pyrolysis parameters (*i.e.*, feedstock type and gaseous medium) for tailoring the biochar physicochemical properties, surface structure, and interfacial chemical behaviour; and (ii) capitalize on the evolution of MW-induced thermal effect for biochar-catalyzed organic removal *via* generation of "hot spots" and various ROSs. The results of this study are conducive to improving the future design of high-efficiency, sustainable, and 'green' engineered carbon catalysts for application of MW irradiation in wastewater treatment.

2. Materials and methods

2.1. Biomass and chemicals

Waste wood biomasses of oak tree and apple tree were collected from Wuxi city (Jiangsu province, China) and Guiyang city (Guizhou province, China), respectively, and were applied as biochar feedstocks without further treatment. All chemicals used in this study (*viz.* 2,4-dichlorophenoxyacetic acid ($C_8H_6Cl_2O_3$, 2,4-D), *tert*-butanol ($C_4H_{10}O$, TBA), chloroform ($CHCl_3$, CF), furfuryl alcohol ($C_5H_6O_2$, FFA), methanol (CH_3OH), ethanol (C_2H_5OH), hexane (C_6H_{14}), acetonitrile (CH_3CN), dimethylsulfoxide ((CH_3)$_2$SO, DMSO), and acetic acid (CH_3COOH)) were of analytical reagent grade and solvents were of high-performance liquid chromatography (HPLC) grade from Sigma-Aldrich Co. Lit. (St. Louis, USA). Ultrapure water (UW, 18.2 MΩ cm), obtained from a Millipore Milli-Q Water Purification System (Milford, USA), was employed for all experimental aqueous solutions.

2.2. Preparation of the biochars

Wood waste (oak tree and apple tree) were cut into small pieces (< 1 cm), crushed and sieved through a 120-mesh (particle size < 0.125 mm), and then pyrolyzed in a tube furnace that was heated to 900 °C at a heating rate of 10 °C min^{-1}, and lasted for 2 h after reaching the target temperature with continuous N_2 or CO_2 purging at a flow rate of 200 mL min^{-1}. After being cooled down to room temperature (23 ±2 °C) inside the furnace, the samples were taken out, ground and passed through a 200-mesh sieve (particle size < 0.075 mm), and stored in airtight containers before use. The obtained oak and apple tree biochars were denoted as OBC-900N, OBC-900C, ABC-900N, and ABC-900C, respectively, where N/C corresponded to N_2/CO_2 purging.

2.3. Characterization of the biochars

The ultimate elemental analysis (EA, Vario EL cube, Germany) was used to estimate the CHONS elemental ratio in the biochar samples. The surface morphology and approximate surface elemental analysis of the obtained biochar samples were observed using scanning electron microscopy coupled with energy-dispersive X-ray spectroscopy (SEM-EDS, JSM-IT300, JXA-8230, Hitachi, Japan). The textural characteristics were determined using N_2 adsorption-desorption isotherms obtained from a surface area analyzer (Quantachrome Autosorb, USA) at 77 K for Brunauer-Emmett-Teller (BET) surface area and Barrett-Joyner-Halenda (BJH) porosity analyses. The Fourier transform infrared (FTIR, Nicolet 6700 spectrometer, USA) spectroscopy was used to observe the near-surface functionalities on biochars with the wavelength range at 400–4000 cm^{-1}. The micro-Raman spectrometer (Raman spectra, Renishwa Invia Fellex, UK) equipped with a Diode-Pumped Solid State (DPSS) at 532 nm excitation was used to record the defective level and graphitization degree of the biochars. The X-ray photoelectron spectroscopy (XPS, Thermo Fisher Scientific, USA) with Al Kα radiation was used to investigate the composition and chemical state of the elements on the sample surfaces. The binding energy of all characteristic peaks were calibrated with carbon C1s core level at 284.8 eV. Devolution of XPS data was conducted using Shirley background associated with Gaussian-Lorentzian model in XPSPEAK41, and the component peaks were identified by comparison of

their binding energies (BEs) with the reported values in the literature.

2.4. MW-assisted removal of 2,4-D by the biochars

The 2,4-D solution was prepared at an initial concentration of 100 mg L^{-1} (in accordance with the average concentration reported in 2,4-D manufacturing wastewaters [41,42]) by dissolving a certain amount of $C_8H_6Cl_2O_3$ in 1 L UW under magnetic stirring at 200 rpm for 6 h. To initiate the reaction, 20 mL of the 2,4-D solution and 20 mg of the biochars (OBC-900N, OBC-900C, ABC-900N, and ABC-900C, respectively) were added in 100 mL Teflon reaction vessels without pH adjustment and heated in the Ethos UP MW Reactor (Milestone, 2450 MHz, maximum power of 1900 W) under continuous magnetic stirring. The biochar loading (*i.e.*, 1 g L^{-1}) was determined according to preliminary experiments (data not shown) for obtaining relatively high 2,4-D removal by the four biochars with distinguishable differences. The MW temperature was ramped from room temperature to 90 °C within 2 min, held for 1 min, and gradually cooled down to below 60 °C by continuous mechanical ventilation in the MW reactor. The adopted reaction temperature and duration were comparable to previous studies on MW-assisted organic removal [20-22]. After reaction, an aliquot of 1 mL solution was withdrawn from the vessels, filtered into HPLC sample vials through 0.45 μm pore-size mixed cellulose ester membrane filters (MCE, Millipore), and tested for 2,4-D concentration by HPLC. The spent biochars were recovered by vacuum filtration, rinsed with UW, and oven dried at 60 °C overnight. The reusability of biochars was investigated by reacting spent samples (1 g L^{-1}) with 20 mL solution of 2,4-D (100 mg L^{-1}) in the MW reactor. A control experiment with only MW and no biochar was conducted. A comparative experiment using oil bath as the heating source was also performed under the same reaction conditions. The adsorption of 2,4-D by biochars was investigated at room temperature. No leaching of metals, organics, or nutrients was detected from the four biochars under the studied experimental conditions.

To verify the *in-situ* formation of radicals, such as $^{\bullet}OH$, anionic superoxide radical ($O_2^{\bullet-}$), and singlet oxygen ($^1O_2$), during MW-assisted removal of 2,4-D, certain quantities of different organic scavengers (TBA

(k_{OH} = (3.2−7.6) × 10^8 M$^{−1}$ s$^{−1}$), CF ($k_{O_2^-}$ = (1.1−3.2) × 10^9 M$^{−1}$ s$^{−1}$), and FFA ($k^t_{O_2}$ = 1.2 × 10^8 M$^{−1}$ s$^{−1}$),

respectively) were doped into the MW vessels to reach the target concentration of 45.2 mmol (at molar ratio

to 2,4-D of 100:1) [39,43], respectively. The radical quenching experiment was conducted under the same

MW/oil bath/room temperature conditions.

To extract adsorbed 2,4-D and possible degradation intermediates, after 1-min reaction in the three systems,

the spent samples were: (i) transferred into 20 mL solution of organic solvent (methanol, ethanol, hexane,

acetonitrile, and DMSO, respectively) under 8-h end-over-end shaking at 30 rpm [40]; or (ii) added into 20

mL mixed solution of water and different organic solvents (50%, *v/v*) under 1-min reaction in MW reactors

at 90 °C [21]. The above solutions were then analyzed for the extracted 2,4-D.

2.5. Analytical methods

The samples were analyzed for 2,4-D by a HPLC (Hitachi Chromaster 5420, Japan, limit of detection

(LOD) of 0.1 mg L$^{−1}$) equipped with an ODS-2 chromatography column (150 mm × 4.6 mm, 5 μm) and an

ultraviolet and visible spectrophotometry (UV-VIS) detector with UV wavelength set at 280 nm [44]. A

mixture of 60% (*v/v* %) acetonitrile, 38% (*v/v* %) UW, and 2% (*v/v* %) acetic acid was used as the mobile

phase at a flow rate of 0.5 mL min$^{−1}$ [44]. The peak for 2,4-D was detected at a retention time of 5.6 min [44].

The total organic carbon (TOC) concentration was measured by a TOC analyzer (Shimadzu, SSM-5000A,

Japan, LOD of 0.1 mg L$^{−1}$). The 2,4-D or TOC removal efficiency was calculated using **Eq. 1** as follows.

Removal efficiency = ($C_{initial}$ − C_{final}) / $C_{initial}$ × 100%   (**Eq.1**)

Standard calibration was carried out prior to each analysis. Standards were analyzed every 10 samples for

quality assurance and quality control. All experiments were performed in at least triplicate, and the results are

presented as mean ± standard deviations. One-way analysis of variance (ANOVA) by the Duncan test was

applied to analyze the significance of differences between data (SPSS version 22.0). The lower-case letters in

the figures represent data grouping based on the significance level of 0.05 (p < 0.05).

3. Results and discussion

3.1. Characterization of the biochars

The distinctive physicochemical properties of the various biochars prepared from different feedstocks under N_2/CO_2 purging are summarized in **Table 1**. Pyrolysis of the lignin-rich biomass (*i.e.,* oak wood) produced biochars (OBC-900N and OBC-900C) with higher yield (20.8 and 19.8%) and carbon content (92.1 and 88.6 *wt.%*). Switching the purging gas from N_2 to CO_2 noticeably lowered the yield (from 19.8 to 17.0%) and carbon content (from 88.8 to 78.9 *wt.%*) of the resultant ABC-900s. These indicated that thermal decomposition of biomass in a CO_2 environment is more significant than that in a N_2 atmosphere, probably due to accelerated consumption of carbon matrix by CO_2 and other active gases produced during pyrolysis [45,46]. The elemental analysis revealed that the OBC-900s exhibited much lower molar ratios of H/C (0.010 of the OBC-900C and 0.011 of the OBC-900N) than the ABC-900s (0.025 of the ABC-900C and 0.079 of the ABC-900N), suggesting an increased biochar aromaticity with higher lignin content in the feedstocks and using CO_2 pyrolysis. The higher molar ratio of (O+N)/C of the ABC-900C (0.200) compared to ABC-900N (0.096) indicated an improved hydrophilicity and polarity in CO_2. In particular, the ABC-900C contained a much higher oxygen content (20.3 *wt.%*) than the other three biochars, probably because of CO_2 induced carbon oxidation during cooling inside the tube furnace after pyrolysis [47]. The zeta potential of the OBC-900s was negative (-18.8 – -12.6 mV) in contrast to the positively charged surfaces of the ABC-900s (2.64 – 6.73 mV), which can be ascribed to the higher metal (*i.e.,* Ca, K, Mg, Na, Fe, and Al) content in the former (**Table 1**). The pH values of the CO_2 pyrolyzed biochars (10.8–10.9) were lower than those of the N_2 pyrolyzed biochars (11.2–12.4), despite their similar ash contents (**Table 1**). CO_2 may have acidified the biochars *via* the creation of more near-surface oxygen-containing functionalities [45,48], which could be verified by the XPS analysis in the subsequent discussion.

The SEM images clearly depict the morphological and structural differences in the biochars dependent on different feedstocks and purging gases (**Fig. 1**). The OBC-900s presented rougher surfaces because of their higher ash content (**Table 1**), while the ABC-900s exhibited more porous structures due to the hierarchical spatial structure of softwood (*e.g.*, apple tree) [23]. As shown in **Fig. 1**, micro- and meso-pores were highly developed inside the carbon matrix of the CO_2 biochars (*i.e.*, OBC-900C and ABC-900C). These were also evidenced by the surface area and pore size distribution of the biochars in **Table 1**. The BET surface area (S_{BET}, 479.9 or 510.5 $m^2\,g^{-1}$) and total pore volume (V_{total}, 0.325 or 0.349 $cm^3\,g^{-1}$) of biochars fabricated in a CO_2 environment (OBC-900C or ABC-900C) were significantly higher than those generated in a N_2 environment. The CO_2 medium promoted the formation of micropores (377.5 or 384.4 $m^2\,g^{-1}$) of the OBC-900C (or ABC-900C). The micropore volume also increased from 0.164 (ABC-900N, 46.8% of V_{total}) to 0.235 (ABC-900C, 67.4% of V_{total}) $cm^3\,g^{-1}$. The average pore diameter (D_p) increased from 2.53 nm for the OBC-900N to 2.90 nm for the OBC-900C, indicating that CO_2 acted as a pore-enlarging agent. Tar and volatile organics generated from an incomplete thermal degradation of lignin could block the pores in biochars [49]. Such pore blocking was suppressed in CO_2, which could expedit tar cracking/reforming *via* the thermo-dynamically favourable Boudouard reaction between the CO_2 and lignin-C (*viz.* $C + CO_2 \rightarrow CO$) at $\geq 720\,°C$ [50], resulting in highly porous biochars [45].

The near-surface chemical functionalities of the biochars were characterized by FTIR analysis, as shown in **Fig. 2**. The small peak at ~3760 cm^{-1} ascribed to the –OH group was present in the spectra of all the biochars except the ABC-900N [51]. The peaks between 1360 and 1450 cm^{-1} are due to the aromatic C=C rings [52,53], whereas the aromatic C–C rings appeared at ~760 cm^{-1} [54]. The high-temperature (900 °C) pyrolysis eliminated the O-containing functional groups from the biochar surface and increased the content of condensed aromatic rings [38,39] as a result of intensive decomposition of the aliphatic and phenolic organic compounds *via* dehydration of cellulosic and ligneous components [39]. Biomass with higher lignin

content in a CO_2 atmosphere can provide biochars with a higher level of carbonization, as evidenced by the increasing intensity of aromatic peaks in the order of ABC-900N < ABC-900C < OBC-900N < OBC-900C (**Fig. 2**), in accordance with the elemental analysis (**Table 1**).

The graphitization degree of the biochars was further investigated by Raman analysis (**Fig. 3**). The Raman spectra of the biochar samples were deconvoluted into five characteristics peaks that were assigned to sp^2 C–H of aromatic rings (S^1) at 1060 cm^{-1}, defect bands and small ordered fused benzene rings (D) at 1310 cm^{-1}, methyl group and amorphous carbon (V^1) at 1380 cm^{-1}, aromatics with 3–5 rings (G^1) at 1540 cm^{-1}, and highly ordered sp^2 graphitic carbon (G) at 1590 cm^{-1}, respectively [39]. The area ratio of the D peak to the G peak (A_D/A_G) of the CO_2 pyrolyzed composites (1.94–2.56) was smaller than that produced in N_2 (2.26–3.52), suggesting that a CO_2 medium induced higher aromaticity and graphitization within the carbon matrix during pyrolysis [45,50]. Higher proportions of the G (11.5–13.0%) and G^1 (2.58–6.72%) bands were formed in the OBC-900s. The ratio of A_D/A_G decreased when there was a larger lignin content in the feedstocks. The cellulose and hemicellulose with branched polymer structure and short side chains form volatile products during pyrolysis of wood biomass, whereas the lignin with complex crosslinking phenolic polymer structure contributes mainly to the biochar production [23]. At pyrolysis temperatures higher than 700 °C, the fragmentation and repolymerization of lignin monomers favour the biochar formation, which could be accelerated in the presence of CO_2 [23]. Thus, the CO_2 enhanced aromaticity could be attributed to accelerated conversion of lignin monomers [44].

XPS analysis was conducted to investigate the transformation of near-surface functional groups in various biochars (**Fig. 4**). For all the samples, the C 1s spectra consisted of three distinctive peaks that were attributed to the presence of aromatic C–C/C=C at 284.8 eV, C–O at 285.8 eV, and π–π* transition in aromatic rings at 288.3 eV, respectively [38]. As shown in **Fig. 4**, the ratio of aromatic C–C/C=C increased from 65.4–66.9%, for ABC-900s to 68.4–68.7% for OBC-900s. This observation reaffirmed the idea of an enhanced conversion

of the crosslinking C structure to condensed aromatic nature of biochars derived from lignin-rich feedstocks [23,39], agreeing with the elemental composition (**Table 1**), FTIR spectra (**Fig. 2**), and Raman spectra (**Fig. 3**). Moreover, by means of XPS analysis, oxygen-containing functional groups (C–O) were identifiable on the biochar surface, the ratio of which increased from 16.1% (ABC-900N) to 17.5% (ABC-900C) after CO_2 activation. This contradictory observation compared with FTIR analysis (**Fig. 2**) might be due to the effect of solution pH and pKa of biochar on the sensitivity of FTIR, which is a bulk technique that reflects the average bonding environment. The C–O might result from the interaction of CO_2 with organic/inorganic compounds in the biochar [49]. Moreover, the density of π–π* transition in aromatic rings increased from 14.7–15.1% in the OBC-900s to 17.0–17.1% in the ABC-900s (**Fig. 4**). According to a previous study [55], these functionalities (C–O and π–π* transition) on biochar could contribute to effective adsorption of 2,4-D. However, it should be acknowledged that the above discussion was mainly based on the peak fitting of XPS spectra, which might be complicated by the small differences between different biochars. More accurate analysis using advanced and computational techniques should also be pursued in future studies.

3.2. MW-assisted removal of 2,4-D by the biochars

Removal efficiencies of 2,4-D by various biochars under three reaction conditions (*i.e.*, room temperature, oil bath, and MW irradiation) are presented and compared in **Fig. 5**. CO_2 activated biochars (ABC-900C and OBC-900C) with increased S_{BET} (479.9 and 510.5 m^2 g^{-1}) and D_p (2.90 and 2.99 nm) gave better 2,4-D adsorption performance than the N_2-produced biochars. CO_2 modification significantly promoted 2,4-D adsorption on OBC-900 and ABC-900, with the equilibrium removal efficiency improved from 40.9 ±0.7 to 49.4 ±7.3% and from 41.8 ±1.5 to 69.8 ±7.0% (**Fig. S1** (**Supporting Information**)) after 30-min reaction, respectively, at room temperature without heating. A previous study also discovered a positive correlation between the specific surface area of biochar (400–600 m^2 g^{-1}) and its 2,4-D adsorption capacity [40],

indicating that the progressive widening of micropores into mesopores accommodated more 2,4-D molecules with polar surface area of 47 Å^2 [40]. Apart from a porous structure, other physicochemical properties of biochar also determined its capacity for 2,4-D adsorption. Our study suggested ABC-900C as the best-performing adsorbent of 2,4-D at room temperature. It had a zeta potential of 2.64 mV **(Table 1)** and thus a positively charged surface that favoured electrostatic interaction with the anionic form of 2,4-D at solution pH > 2.7 [55]. In addition, biochars with higher content of the π–π* transition (17.1% of the ABC-900C, **Fig. 4**) as electron acceptor could strengthen attraction with the electron-rich benzene ring of 2,4-D as electron donor *via* π–π interaction [55]. Moreover, the abundant oxygen-containing functional groups (17.5% C–O, **Fig. 4**) in the ABC-900C could contribute more active sites for 2,4-D adsorption [55]. Thus, adsorption of 2,4-D by biochar was likely a result of electrostatic interaction, electron conjugation, and chemisorption [55].

The significantly promoted removal of 2,4-D under MW irradiation is clearly illustrated in **Fig. 5**. After 1-min reaction in the MW reactor, 2,4-D removal by the OBC-900C and OBC-900N was obviously increased to 81.6 ±0.8 and 57.4 ±4.1%, respectively, *i.e.*, ~2.3 times the removal efficiency under room temperature. No 2.4-D removal was observed under MW irradiation only in the absence of biochar due to the low volatility of 2,4-D. However, gas emission could be a potential problem of the MW system for semi-volatile and volatile contaminants. MW treatment outperformed conventional heating in an oil bath at the same reaction temperature (90 °C) for 1–30 min (**Fig. 5** and **Fig. S1**). In particular, the OBC-900C, which achieved the highest removal in MW, consumed less energy than the rest of the biochars during the temperature ramping (1.39 *vs.* 1.68 kW) and holding (0.275 *vs.* 0.601 kW) stages, despite the same heating programme (**Fig. 6**). This suggested a more efficient MW-to-thermal energy transformation over the MW-absorbing OBC-900C. Furthermore, its temperature profile showed overshooting (~1 °C) after the ramping, which was absent from the other biochars. The strong MW absorptivity of the OBC-900C might have induced localized overheating, which promoted the removal of 2,4-D. Thus, the OBC-900C could absorb maximal electromagnetic energy

that ultimately penetrates into its carbon matrix and quickly dissipate as heat or other forms of energy [4].

There was only a slight improvement of 2,4-D removal in the presence of the ABC-900C under MW irradiation (69.9 ±1.7%) compared to oil bath heating (62.4 ±0.6%), both of which were better than room-temperature treatment (52.6 ±4.2%) (**Fig. 5**). In addition, the OBC-750C (pyrolyzed at a lower temperature of 750 °C) exhibited a significantly inferior performance for 2,4-D removal under the three different reaction conditions (**Fig. 5**). These results indicate that biochar prepared from various feedstocks, purging gases, and pyrolysis temperatures exhibited a distinctive sensitivity to MW irradiation. Carbon materials have been explored as MW adsorbents due to their high dielectric loss that is usually dependent on two critical factors, the bonding state of carbon atoms (*i.e.*, degree of graphitization) and the microstructure of the carbon matrix [16]. On one hand, the large surface area ($S_{BET} = 510.5 \text{ m}^2 \text{ g}^{-1}$), high proportion of micropores ($V_{micro}/V_{total} = 67.4\%$), appropriate pore size ($D_p = 2.99$ nm), and abundant surface functionalities (17.5% C–O and 17.1% π–π* transition in aromatic rings) of the ABC-900C could guarantee sufficient adsorption of aquatic organic pollutants (**Table 1** and **Fig. 4**). On the other hand, the higher degree of graphitization of the OBC-900C ($A_D/A_G = 1.94$ and 68.7% aromatic C–C/C=C, **Figs. 3-4**), together with its greater microwave absorbing property and medium-developed microporous structure, would be beneficial to the capture and degradation of 2,4-D under MW irradiation.

The MW-enhanced organic removal may also be attributed to the formation of various ROSs catalyzed by the carbon surface [21]. As shown in **Fig. 7**, TBA addition only slightly decreased the 2,4-D removal to 34.2 ±0.8% by the ABC-900N while performances of the other biochars remained unaffected. In contrast, CF or FFA noticeably inhibited the 2,4-D removal to the same extent in the MW systems containing the OBC-900C and ABC-900C (44.5 ±5.6 − 52.8 ±0.7% and 20.4 ±0.4 − 22.3 ±4.2%, respectively) compared with 81.6 ±0.8 and 61.9 ±1.7% removal with no scavengers (**Fig. 7**), indicating the equal contribution of $O_2^{\bullet-}$ and $^1O_2$ to 2,4-D removal. However, in the case of N_2 pyrolyzed biochars , FFA led to a more significant decrease in 2,4-D

removal compared with CF, *i.e.,* 49.1 ±4.9 *vs.* 36.6 ±0.3% and 10.5 ±2.6 *vs.*3.1 ±0.8% for the OBC-900N and ABC-900N, respectively (**Fig. 7**), suggesting that $^1O_2$ played a superior role than the other ROSs. In particular, the additional organic scavengers did not exhibit noticeable effect on 2,4-D removal under room temperature or oil bath conditions. This observation excluded the potential interference of these organic scavengers on 2,4-D adsorption, and reaffirmed that radicals were only generated in the MW system. The production of radical species is summarized in reactions **R1–R3** according to previous studies [23]. Upon MW irradiation, water (H_2O) molecules surrounding biochar surface "hot spots" could be activated into $^{\bullet}OH$ and hydrogen radicals ($^{\bullet}H$) (**R1**). Oxygen (O_2) in the water medium would react with $^{\bullet}H$ to form $O_2^{\bullet -}$ and $^1O_2$ (**R2**), which could further yield $^{\bullet}OH$ *via* **R3**. These radicals ($O_2^{\bullet -}$ and $^1O_2$) with powerful oxidization capacity could decompose the adsorbed or soluble 2,4-D into intermediates with lower molecular weight, and finally mineralize into CO_2 and H_2O.

$$H_2O \xrightarrow{MW} {^{\bullet}OH} + {^{\bullet}H} \tag{R1}$$

$$2O_2 + {^{\bullet}H} \xrightarrow{MW} {^1O_2} + O_2^{\bullet -} + H^+ \tag{R2}$$

$$O_2^{\bullet -} + 2H_2O \xrightarrow{MW} 3{^{\bullet}OH} + OH^- \tag{R3}$$

3.3. Desorption and reusability of the biochars

To further distinguish adsorption and degradation of 2,4-D under the three reaction conditions (MW irradiation, oil bath, and room temperature), the adsorbed 2,4-D on the spent biochars were extracted by different organic solvents (methanol, ethanol, hexane, acetonitrile, and DMSO respectively) *via* desorption at room temperature and under MW conditions, respectively. However, neither desorption procedures with any organic solvent could recover more than 10% 2,4-D from the reacted samples. These results might be due to strong binding between 2,4-D and biochar *via* diffusion into the inner porous structure and intensive chemisorption by the surface functionalities of biochar [40]. In addition, the 1-min TOC removal (59.2 ±2.5,

43.3 ±0.9, 83.0 ±3.4, and 71.9 ±3.2%, respectively) by the OBC-900N, ABC-900N, OBC-900C, and ABC-900N, respectively, was slightly greater than the 2,4-D removal (57.4 ±4.1, 41.2 ±2.2, 81.6 ±0.8, and 69.9 ±1.7%, respectively) under MW conditions (**Fig. S2**). These results indicated that 2,4-D could be completely mineralized into CO_2 and H_2O by the MW-assisted removal in presence of biochar. Moreover, no obvious peaks of any degradation intermediates were observed by HPLC analysis of the solutions after reaction or the extraction solutions of the spent biochars, probably because of a strong entrapment of possible by-products by the biochars. Thus, no direct evidence of 2,4-D decomposition (within the accuracies of the experimental methods) could be provided in the current stage of our study. According to the latest findings [56], the dechlorination rate of 2,4-D (*i.e.*, change of the Cl^- concentration) was correlated to its degradation efficiency when 2,4-D was completely mineralized into CO_2 and H_2O. More comprehensive experimental design (*e.g.*, extraction of reacted biochars by other means, full identification of 2,4-D intermediates, and detection of released Cl^-) would help to further prove and quantify the 2,4-D degradation in the MW/biochar system.

Reusability of the OBC-900N and OBC-900C biochars was tested in three consecutive cycles of 2,4-D removal under MW irradiation. A progressive loss of biochar activity in each cycle is depicted in **Fig. 8**. Without any treatment of regeneration, the performance of the OBC-900C (or OBC-900N) noticeably dropped from 81.7 ±2.1% (or 61.2 ±0.9%) to 24.2 ±1.3% (or 21.2 ±1.1%) 2,4-D removal. This observation could be ascribed to the high BET surface area and internal microporous structure of biochar. The degradation by-products might accumulate and occupy the active sites on biochar surface for 2,4-D adsorption. It is also possible that the carbon materials eventually crumble when "hot spots" formed inside micropores generate sufficient confined vapour with increased pressure [6]. This so-called "popcorn effect" could impede biochar stability with susceptible deactivation and fouling by intermediates [6]. Future studies should focus on biochar regeneration *via* facile and low-cost treatment, for example, low-temperature heating in N_2 environment or desorption by various types of green solvents.

For future design of more sustainable water/wastewater treatment processes, MW technology can be effectively incorporated with membrane bioreactors and electro-/photo-catalysis process [3,4]. However, most current studies on MW system for water/wastewater treatment are conducted in laboratory scale, because (i) volume and power output of the available MW reactors are insufficient for widespread commercial promotion, and (ii) low-cost, highly efficient, and recyclable catalysts are critical for industrial applications [3,4]. With further development of equipment optimization and catalysts exploitation, MW technology is expected to deliver good benefits for practical water and wastewater treatment.

Conclusions

This study has demonstrated that biochar derived from waste biomass of oak tree, with high lignin content under 900 °C pyrolysis and CO_2 purging, can act as a 'green', highly efficient MW absorber. The CO_2 purging can promote decomposition of lignin carbon at high pyrolysis temperature *via* fragmentation and repolymerization, producing biochar with a developed hierarchical porous structure, enhanced graphitization level, and improved surface chemistry. Under mild MW irradiation, 2,4-D was simultaneously adsorbed (*via* electrostatic interaction, electron conjugation, and chemisorption) and degraded due to a MW-induced thermal effect on the biochar surface that generated hydroxyl ($^{•}OH$), anionic superoxide ($O_2^{•-}$), and singlet oxygen ($^{1}O_2$) radicals. This study has demonstrated the potential application of an economical, sustainable, metal-free biochar in energy-saving, chemical-free water/wastewater treatment using MW, which could make an important contribution to a clean water environment. Future studies are suggested to optimize the rational design of MW-active biochar catalysts and investigate the applicability of the MW/biochar system to a broader range of organic pollutants with diverse physicochemical properties in water/wastewater matrices.

References

[1] Sun, J., Pan, L., Tsang, D.C.W., Zhan, Y., Zhu, L., Li, X.D., Organic contamination and remediation in the agricultural soils of China: A critical review, Science of the Total Environment, 615 (2018), 724-740.

[2] Kümmerer, K., Dionysiou, D.D., Olsson, O., Fatta-Kassinos, D., A path to clean water. Science, 361 (2018), 222-224.

[3] Wei, R., Wang, P., Zhang, G., Wang, N., Zheng, T., Microwave-responsive catalysts for wastewater treatment: A review, Chemical Engineering Journal, (2020), 122781.

[4] Xue, C., Mao, Y., Wang, W., Song, Z., Zhao, X., Sun, J., Wang, Y., Current status of applying microwave-associated catalysis for the degradation of organics in aqueous phase-A review, Journal of Environmental Sciences, 81 (2019), 119-135.

[5] Varisli, D., Korkusuz, C., Dogu, T., Microwave-assisted ammonia decomposition reaction over iron incorporated mesoporous carbon catalysts., Applied catalysis B: Environmental, 201 (2017), 370-380.

[6] Garcia-Costa, A.L., Zazo, J.A., Rodriguez, J.J., Casas, J.A., Intensification of catalytic wet peroxide oxidation with microwave radiation: activity and stability of carbon materials, Separation and Purification Technology, 209 (2019), 301-306.

[7] Hu, L., Wang, P., Shen, T., Wang, Q., Wang, X., Xu, P., Zheng, Q., Zhang, G., The application of microwaves in sulfate radical-based advanced oxidation processes for environmental remediation: A review, Science of The Total Environment, (2020), 137831.

[8] Garcia-Costa, A.L., Zazo, J.A., Rodriguez, J.J., Casas, J.A., Microwave-assisted catalytic wet peroxide oxidation. Comparison of Fe catalysts supported on activated carbon and γ-alumina, Applied Catalysis B:

Environmental, 218 (2017), 637-642.

[9] Chen, J., Pan, H., Hou, H., Li, H., Yang, J., Wang, L., High efficient catalytic degradation of PNP over Cu-bearing catalysts with microwave irradiation, Chemical Engineering Journal, 323 (2017), 444-454.

[10] Wang, X., Mei, L., Xing, X., Liao, L., Lv, G., Li, Z., Wu, L., Mechanism and process of methylene blue degradation by manganese oxides under microwave irradiation, Applied Catalysis B: Environmental, 160 (2014), 211-216.

[11] Ahmed, A. B., Jibril, B., Danwittayakul, S., Dutta, J., Microwave-enhanced degradation of phenol over Ni-loaded ZnO nanorods catalyst, Applied Catalysis B: Environmental, 156 (2014), 456-465.

[12] Ling, L., Feng, Y., Li, H., Chen, Y., Wen, J., Zhu, J., Bian, Z., Microwave induced surface enhanced pollutant adsorption and photocatalytic degradation on Ag/TiO$_2$, Applied Surface Science, 483 (2019), 772-778.

[13] Qi, Y., Mei, Y., Li, J., Yao, T., Yang, Y., Jia, W., Tong, X., Wu, J., Xin, B., Highly efficient microwave-assisted Fenton degradation of metacycline using pine-needle-like CuCo$_2$O$_4$ nanocatalyst, Chemical Engineering Journal, 373 (2019), 1158-1167.

[14] Qiu, Y. and Zhou, J., Highly effective and green microwave catalytic oxidation degradation of nitrophenols over Bi$_2$O$_2$CO$_3$ based composites without extra chemical additives, Chemosphere, 214 (2019), 319-329.

[15] Yao, X., Lin, Q., Zeng, L., Xiang, J., Yin, G., & Liu, Q. (2017). Degradation of humic acid using hydrogen peroxide activated by CuO-Co$_3$O$_4$@ AC under microwave irradiation. Chemical Engineering Journal, 330, 783-791.

[16] Cai, B., Feng, J. F., Peng, Q. Y., Zhao, H. F., Miao, Y. C., Pan, H., Super-fast degradation of high concentration methyl orange over bifunctional catalyst Fe/Fe$_3$C@C with microwave irradiation, Journal of Hazardous Materials, 392 (2020), 122279.

[17] Yao, T., Qi, Y., Mei, Y., Yang, Y., Aleisa, R., Tong, X., Wu, J., One-step preparation of reduced graphene oxide aerogel loaded with mesoporous copper ferrite nanocubes: A highly efficient catalyst in microwave-assisted Fenton reaction, Journal of Hazardous mMaterials, 378 (2019), 120712.

[18] Shen, M., Fu, L., Tang, J., Liu, M., Song, Y., Tian, F., Zhao, Z., Zhang, Z., Dionysiou, D.D., Microwave hydrothermal-assisted preparation of novel spinel-NiFe$_2$O$_4$/natural mineral composites as microwave catalysts for degradation of aquatic organic pollutants, Journal of Hazardous Materials, 350 (2018), 1-9.

[20] Zhang, Z., Shan, Y., Wang, J., Ling, H., Zang, S., Gao, W., Zhao, Z., Zhang, H., Investigation on the rapid degradation of congo red catalyzed by activated carbon powder under microwave irradiation, Journal of Hazardous Materials, 147 (2007), 325-333.

[21] Veksha, A., Pandya, P., Hill, J.M., The removal of methyl orange from aqueous solution by biochar and activated carbon under microwave irradiation and in the presence of hydrogen peroxide, Journal of Environmental Chemical Engineering, 3 (2015), 1452-1458.

[22] Chen, J., Xue, S., Song, Y., Shen, M., Zhang, Z., Yuan, T., Tian, F., Dionysiou, D.D., Microwave-induced carbon nanotubes catalytic degradation of organic pollutants in aqueous solution, Journal of Hazardous Materials, 310 (2016), 226-234.

[23] Rangabhashiyam, S. and Balasubramanian, P., The potential of lignocellulosic biomass precursors for biochar production: performance, mechanism and wastewater application-A review, Industrial Crops and Products, 128 (2019), 405-423.

[24] Kumar, M., Xiong, X., Sun, Y., Iris, K.M., Tsang, D.C.W., Hou, D., Gupta, J., Bhaskard, T., Pandey, A., Critical review on biochar-supported catalysts for pollutant degradation and sustainable biorefinery. Advanced Sustainable Systems, (2020), 1900149.

[25] Shaheen, S.M., Niazi, N.K., Hassan, N.E., Bibi, I., Wang, H., Tsang, D.C.W., Ok., Y.S., Bolan, N., Rinklebe, J., Wood-based biochar for the removal of potentially toxic elements in water and wastewater:

a critical review, International Materials Reviews, 64 (2019), 216-247.

[26] El-Naggar, A., Lee, S.S., Awad, Y.M., Yang, X., Ryu, C., Rizwan, M., Rinklebe, J., Tsang, D.C.W., Ok, Y.S., Influence of soil properties and feedstocks on biochar potential for carbon mineralization and improvement of infertile soils, Geoderma, 332 (2018), 100-108.

[27] Igalavithana, A.D., Lee, S.E., Lee, Y.H., Tsang, D.C.W., Rinklebe, J., Kwon, E.E., Ok, Y.S., Heavy metal immobilization and microbial community abundance by vegetable waste and pine cone biochar of agricultural soils, Chemosphere, 174 (2017), 593-603.

[28] Dissanayake, P.D., Choi, S.W., Igalavithana, A.D., Yang, X., Tsang, D.C.W., Wang, C.H., Kua, H.W., Lee, K.B., Ok, Y.S., Sustainable gasification biochar as a high efficiency adsorbent for CO_2 capture: A facile method to designer biochar fabrication, Renewable and Sustainable Energy Reviews, 124 (2020), 109785.

[29] Xu, X., Xu, Z., Gao, B., Zhao, L., Zheng, Y., Huang, J., Tsang, D.C.W., Ok, Y.S., Cao, X., New insights into CO_2 sorption on biochar/Fe oxyhydroxide composites: Kinetics, mechanisms, and in situ characterization, Chemical Engineering Journal, 384 (2020), 123289.

[30] Sun, Y., Chen, S.S., Lau, A.Y.T., Tsang, D.C.W., Mohanty, S.K., Bhatnagar, A., Rinklebe, J., Lin, A.K.Y., Ok, Y.S. Waste-derived compost and biochar amendments for stormwater treatment in bioretention column: Co-transport of heavy metals and colloid, Journal of Hazardous Materials, 383 (2020), 121243.

[31] Rajapaksha, A.U., Alam, M.S., Chen, N., Alessi, D.S., Igalavithana, A.D., Tsang, D.C.W., Ok, Y.S., Removal of hexavalent chromium in aqueous solutions using biochars: Chemical and spectroscopic investigations. Science of the Total Environment, 625 (2018), 1567-1573.

[32] Ruan, X., Sun, Y., Du, W., Tang, Y., Liu, Q., Zhang, Z., William, D., Ray L.F., Qian, R., Tsang, D.C.W., Formation, characteristics, and application of environmentally persistent free radicals (EPFRs) in biochars and environmental matrices: A Review, Bioresource Technology, 281 (2019), 457-468.

[33] Li, Z., Sun, Y., Yang, Y., Han, Y., Wang, T., Chen, J., Tsang, D.C.W., Biochar-supported nanoscale zero-valent iron as an efficient catalyst for organic degradation in groundwater, Journal of Hazardous Materials, 383 (2020), 121240.

[34] Yu, I.K.M., Xiong, X., Tsang, D.C.W., Wang, L., Hunt, A.J., Song, H., Shang, J., Ok, Y.S., Poon, C.S., Aluminium-biochar composite as a sustainable heterogeneous catalyst for glucose isomerization in biorefinery, Green Chemistry, 21 (2019), 1267-1281.

[35] Xiong, X., Yu, I.K.M., Cao, L., Tsang, D.C.W., Zhang, S., Ok, Y.S., A review of biochar-based catalysts for chemical synthesis, biofuel production, and pollution control. Bioresource Technology, 246 (2017), 254-270.

[36] Mian, M.M., Liu, G., Fu, B., Conversion of sewage sludge into environmental catalyst and microbial fuel cell electrode material: A review, Science of The Total Environment, 666 (2019), 525-539.

[37] Sun, C., Chen, T., Huang, Q., Zhan, M., Li, X., Yan, J., Activation of persulfate by CO_2-activated biochar for improved phenolic pollutant degradation: Performance and mechanism, Chemical Engineering Journal, 380 (2020), 122519.

[38] Sun, Y., Yu, I.K.M., Tsang, D.C.W., Cao, X.D, Lin, D.H, Wang, L.L, Graham, N.J.D., Daniel, S.A., Michael, K., Ok, Y.S., Feng, Y.J., Li, X.D. Multifunctional iron-biochar composites for the removal of potentially toxic elements, inherent cations, and hetero-chloride from hydraulic fracturing wastewater, Environment International, 124 (2019), 521-532.

[39] Wan, Z., Sun, Y., Tsang, D.C.W., Yu, I.K.M., Fan, J., Clark, J.H., Zhou, Y., Cao, X., Gao, B., Ok, Y.S., Sustainable biochar catalyst synergized with copper heteroatoms and CO_2 for singlet oxygenation and electron transfer routes, Green Chemistry, 21 (2019), 4800.

[40] Mandal, S., Sarkar, B., Igalavithana, A.D., Ok, Y.S., Yang, X., Lombi, E., Bolan, N., Mechanistic insights of 2, 4-D sorption onto biochar: Influence of feedstock materials and biochar properties, Bioresource

Technology, 246 (2017), 160-167.

[41] Tiwari, B., Sellamuthu, B., Ouarda, Y., Drogui, P., Tyagi, R.D., Buelna, G., Review on fate and mechanism of removal of pharmaceutical pollutants from wastewater using biological approach, Bioresource Technology, 224 (2017), 1-12.

[42] Shi, X., Leong, K.Y., Ng, H.Y., Anaerobic treatment of pharmaceutical wastewater: a critical review. Bioresource Technology, 245 (2017), 1238-1244.

[43] Wang, D., Sun, Y., Tsang, D.C.W., Khan, E., Cho, D.W., Zhou, Y., Qi, F., Gong, J., Wang, L., Synergistic utilization of inherent halides and alcohols in hydraulic fracturing wastewater for radical-based treatment: A case study of di-(2-ethylhexyl) phthalate removal, Journal of Hazardous Materials, 384 (2020), 121321.

[44] Cho, D.W., Yoon, K., Ahn, Y., Sun, Y., Tsang, D.C.W., Hou, D., Ok, Y.S., Song, H., Fabrication and environmental applications of multifunctional mixed metal-biochar composites (MMBC) from red mud and lignin wastes, Journal of Hazardous Materials, 374 (2019), 412-419.

[45] Lee, J., Yang, X., Cho, S.H., Kim, J.K., Lee, S.S., Tsang, D.C.W., Ok, Y.S., Kwon, E.E., Pyrolysis process of agricultural waste using CO_2 for waste management, energy recovery, and biochar fabrication. Applied Energy, 185 (2017), 214-222.

[46] Qian, F., Zhu, X., Liu, Y., Hao, S., Ren, Z.J., Gao, B., Zong, R., Zhang, S., Chen, J., Synthesis, characterization and adsorption capacity of magnetic carbon composites activated by CO_2: implication for the catalytic mechanisms of iron salts, Journal of Materials Chemistry A, 4 (2016), 18942-18951.

[47] Yang, X., Yu, I.K.M., Cho, D.W., Chen, S.S., Tsang, D.C.W., Shang, J., Yip, A.C.K., Wang, L., Ok, Y.S., Tin-functionalized wood biochar as a sustainable solid catalyst for glucose isomerization in biorefinery, ACS Sustainable Chemistry & Engineering, 7 (2019), 4851-4860.

[48] Liu, Y., Zhu, X., Wei, X., Zhang, S., Chen, J., Ren, Z. J., CO_2 activation promotes available carbonate

and phosphorus of antibiotic mycelial fermentation residue-derived biochar support for increased lead immobilization, Chemical Engineering Journal, 334 (2018), 1101-1107.

[49] Igalavithana, A.D., Yang, X., Zahra, H.R., Tack, F.M., Tsang, D.C.W., Kwon, E.E., Ok, Y.S., Metal (loid) immobilization in soils with biochars pyrolyzed in N_2 and CO_2 environments, Science of the total environment, 630 (2018), 1103-1114.

[50] Kim, Y., Oh, J.I., Vithanage, M., Park, Y.K., Lee, J., Kwon, E.E., Modification of biochar properties using CO_2, Chemical Engineering Journal, 372 (2019), 383-389.

[51] Peng, Y., Sun, Y., Sun, R., Zhou, Y., Tsang, D.C.W., Chen, Q., Optimizing synthesis of Fe/Al (hydr)oxides-biochars to maximize phosphorus removal via response surface model, Journal of Cleaner Production, 237 (2019), 117770.

[52] Yang, F., Zhang, S., Sun, Y., Cheng, K., Li, J., Tsang, D.C.W., Fabrication and characterization of hydrophilic corn stalk biochar-supported nanoscale zero-valent iron composites for efficient metal removal, Bioresource Technology, 265 (2018), 490-497.

[53] Yang, F., Zhang, S., Sun, Y., Tsang, D.C.W., Cheng, K., Ok, Y.S., Assembling biochar with various layered double hydroxides for enhancement of phosphorus recovery, Journal of Hazardous Materials, 365 (2019), 665-673.

[54] Yang, F., Zhang, S., Sun, Y., Du. Q., Song J.P., Tsang, D.C.W., A novel electrochemical modification combined with one-step pyrolysis for preparation of sustainable thorn-like iron-based biochar composites, Bioresource Technology, 274 (2019), 379-385.

[55] Zhu, L., Zhao, N., Tong, L., Lv, Y., Li, G., Characterization and evaluation of surface modified materials based on porous biochar and its adsorption properties for 2, 4-dichlorophenoxyacetic acid, Chemosphere, 210 (2018), 734-744.

[56] Li, W., Li, Y., Zhang, D., Lan, Y., Guo, J., CuO-Co_3O_4@CeO_2 as a heterogeneous catalyst for efficient

degradation of 2, 4-dichlorophenoxyacetic acid by peroxymonosulfate, Journal of Hazardous Materials, 381 (2020), 121209.

List of Table

Table 1. Physicochemical characteristics of various biochars.

Table 1. Physicochemical characteristics of various biochars.

Elemental Compositions	OBC-900N	ABC-900N	OBC-900C	ABC-900C
[a] C (%)	92.1	88.8	88.6	78.9
[a] H (%)	0.082	0.585	0.077	0.164
[a] O (%)	7.67	10.8	11.1	20.3
[a] N (%)	0.165	N.D.	0.203	0.642
[a] S (%)	N.D.	N.D.	N.D.	N.D.
H/C	0.011	0.079	0.010	0.025
(O+N)/C	0.064	0.091	0.096	0.200
[b] Ca (%)	0.06	0.49	0.04	0.50
[b] K (%)	0.06	0.14	0.05	0.14
[b] Mg (%)	0.01	0.05	0.01	0.05
[b] Na (%)	0.01	0.02	N.D.	0.02
[b] Fe (%)	0.01	0.02	0.01	0.01
[b] Al (%)	N.D.	0.04	0.01	0.02
Chemical Properties	**OBC-900N**	**ABC-900N**	**OBC-900C**	**ABC-900C**
[c] pH	11.2	12.4	10.8	10.9
[d] Zeta potential (mV)	-12.6	6.73	-18.8	2.64
Physical Properties	**OBC-900N**	**ABC-900N**	**OBC-900C**	**ABC-900C**
Yield	20.8	19.8	19.8	17.0
BET surface area, S_{BET} ($m^2\,g^{-1}$)	432.0	435.2	479.9	510.5
Micropore surface area, S_{micro} ($m^2\,g^{-1}$)	259.4	276.1	377.5	384.4
External surface area, S_{ext} ($m^2\,g^{-1}$)	172.6	159.1	102.4	122.1
Total pore volume, V_{total} ($cm^3\,g^{-1}$)	0.304	0.313	0.325	0.349
Micropore volume, V_{micro} ($cm^3\,g^{-1}$)	0.132	0.164	0.194	0.235
V_{micro}/V_{total} (%)	43.3	46.8	59.6	67.4
Average pore diameter, D_p (nm)	2.53	2.73	2.90	2.99

[a] Determined by elemental analysis (O wt.% = 100% - C wt.% - H wt.% - N wt.% - ash wt.%).

[b] Determined by total digestion (HNO_3 + $HClO_4$) and inductively coupled plasma atomic emission spectroscopy (ICP-AES, Thermo Scientific, LOD of 0.1 µg L^{-1}) analysis.

[c] 1 g solid + 20 mL DIW, 4-h end-over-end rotation (30 rpm), centrifugation (4000 rpm, 10 min).

[d] 0.25 g solid + 25 mL DIW, 30-min sonication, determined by DLS Zetasizer.

N.D.: Non detectable.

List of Figures

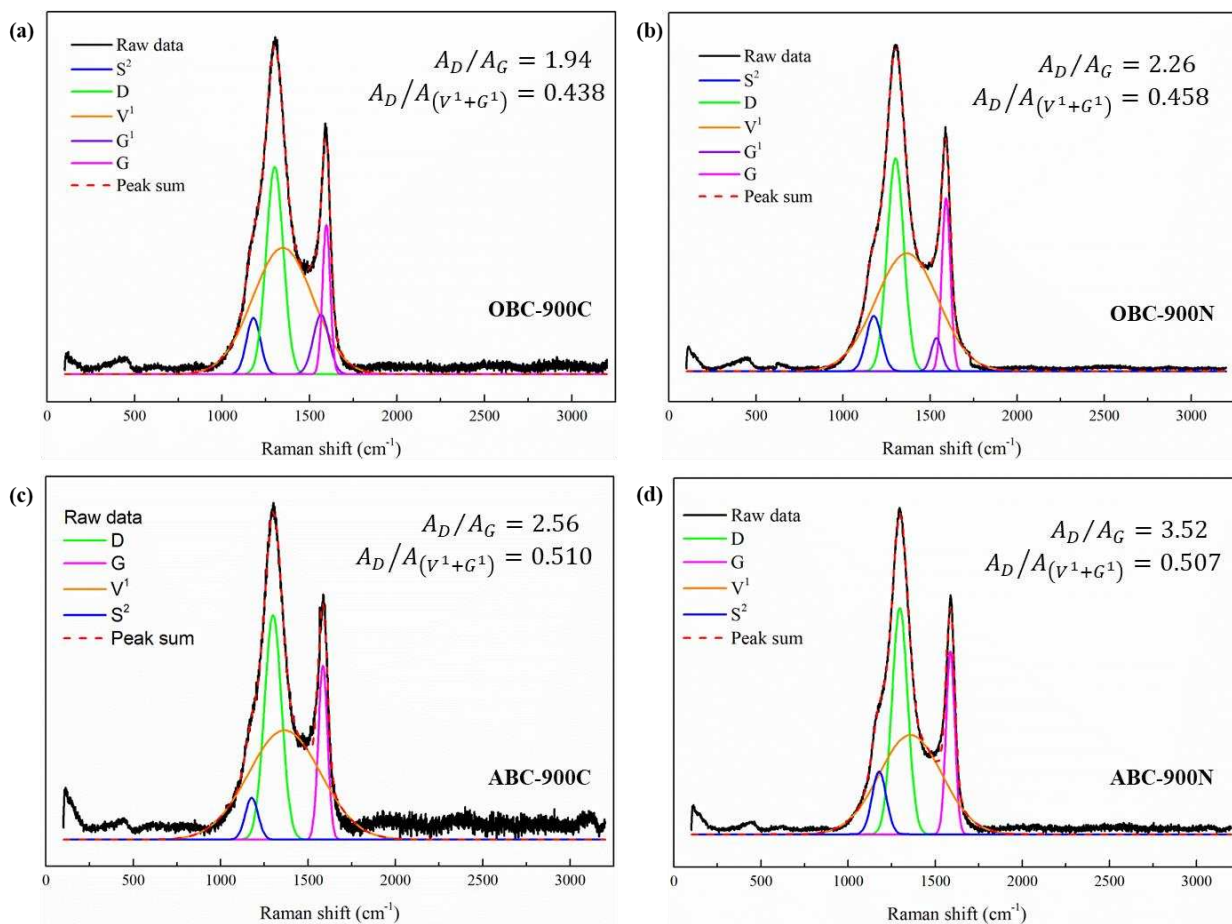| OBC-900N	ABC-900N	OBC-900C	ABC-900C

**Fig. 1.** SEM images of various biochars (a-d: 5,000× magnification; e-h: 20,000× magnification).
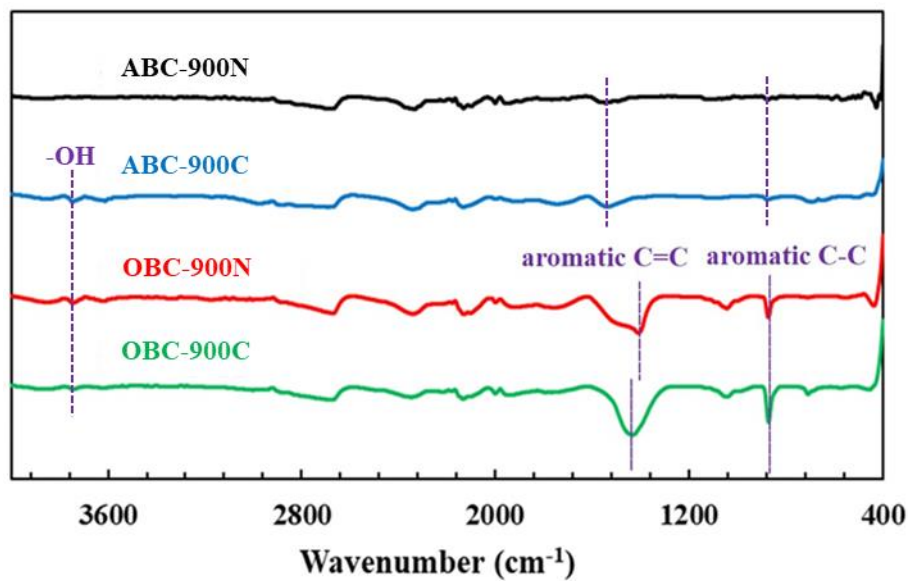
Fig. 2. FTIR spectra of various biochars (3760, 1360–1450, and 760 cm^{-1} assigned to the –OH group, aromatic C=C rings, and aromatic C–C rings, respectively).

Fig. 3. Deconvoluted Raman analysis of various biochars (1230, 1310, 1380, 1540, and 1590 cm^{-1} assigned to arylalkyl ether (S^2), defect bands and small ordered fused benzene rings (D), methyl group and small amorphous carbon (V^1), aromatics with 3–5 rings (G^1), and highly ordered *sp^2* graphitic carbon (G), respectively).
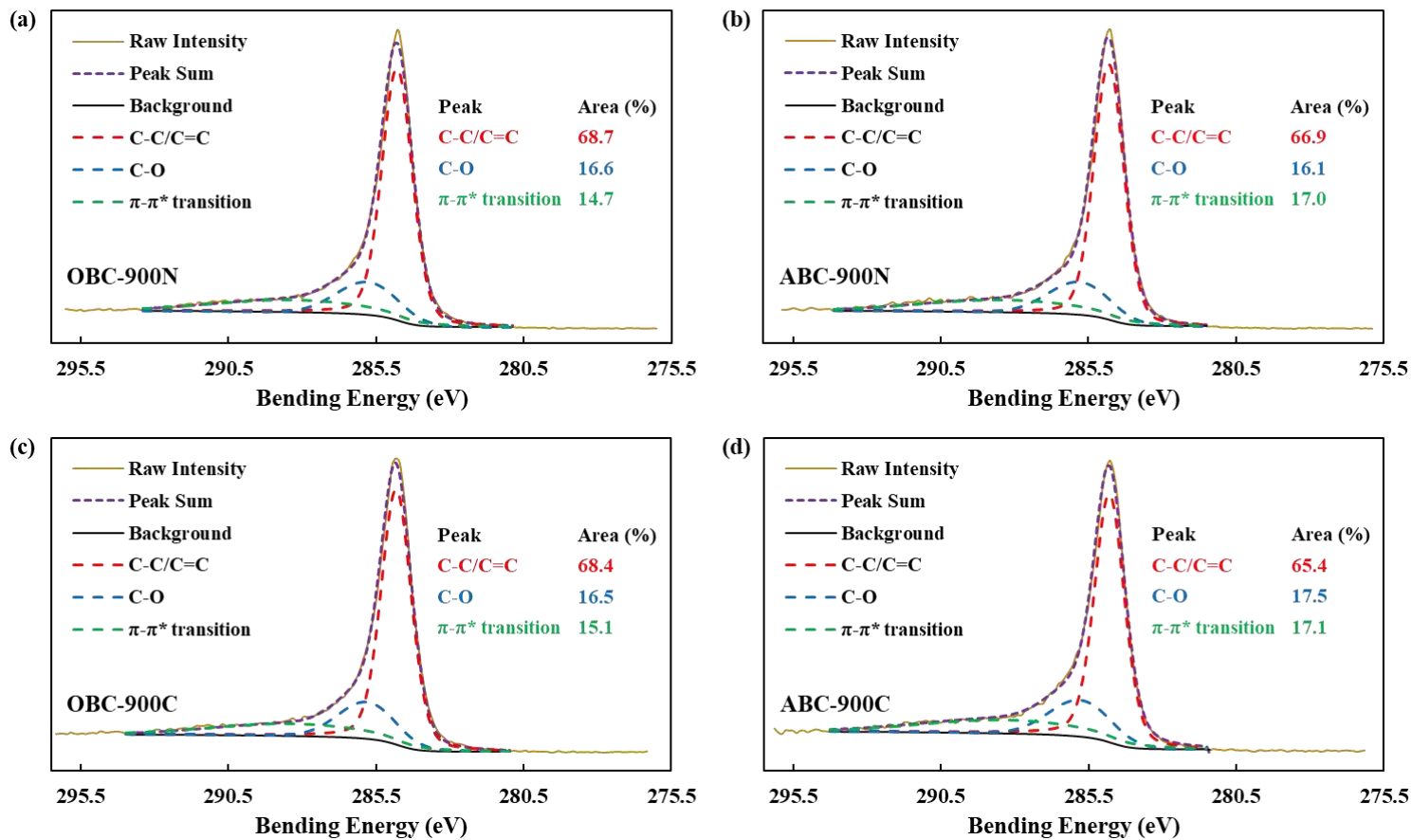
Fig. 4. Deconvoluted XPS analysis of C1s binding states of various biochars (284.8, 285.8, and 288.3 eV assigned to C–C/C=C, C–O, and π–π* transition in aromatic rings, respectively).
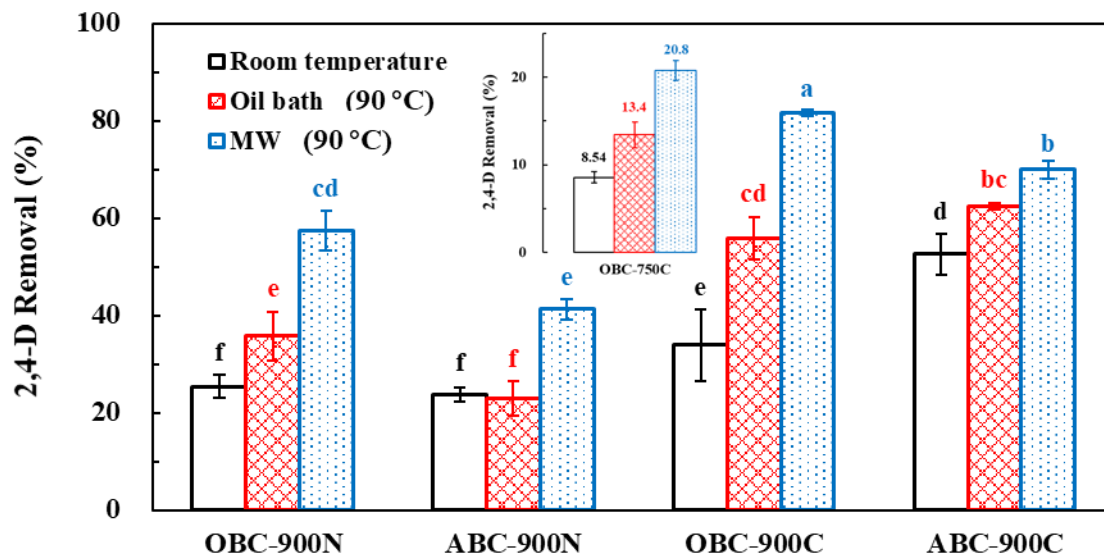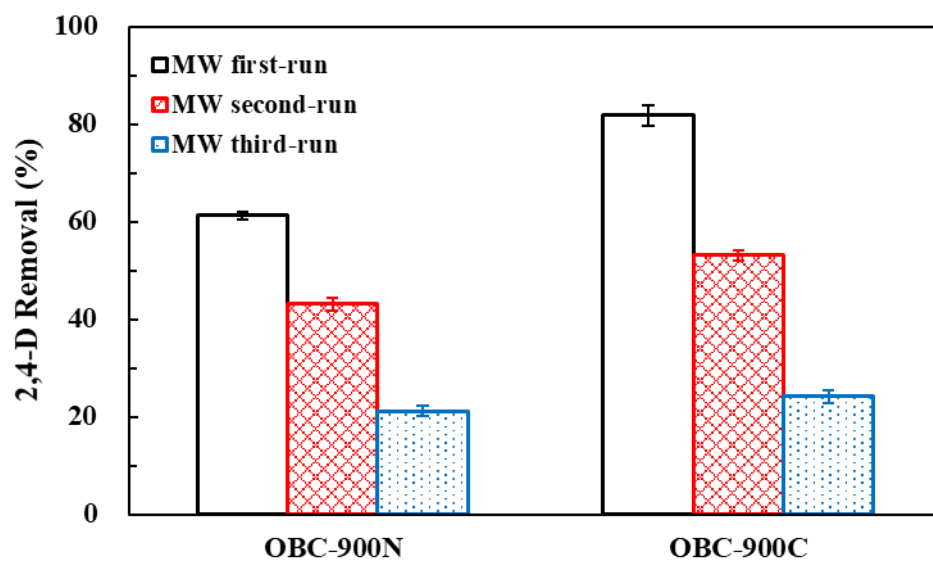
Fig. 5. 2,4-D removal efficiency of various biochars after 1-min reaction in the three systems (Reaction conditions: 2,4-D = 100 mg L^{-1}, biochar = 1 g L^{-1}, V$_{solution}$ = 20 mL, and n = 3; room temperature: 23 ±2 °C; oil bath: temperature increased from 23 ±2 °C to 90 °C in 20 min and hold for 1 min; microwave (MW): temperature increased from 23 ±2 °C to 90 °C in 2 min and hold for 1 min, MW$_{max}$ = 1500W) (lower-case letters indicate the significance levels ($p < 0.05$) of differences in the results of the four biochars).
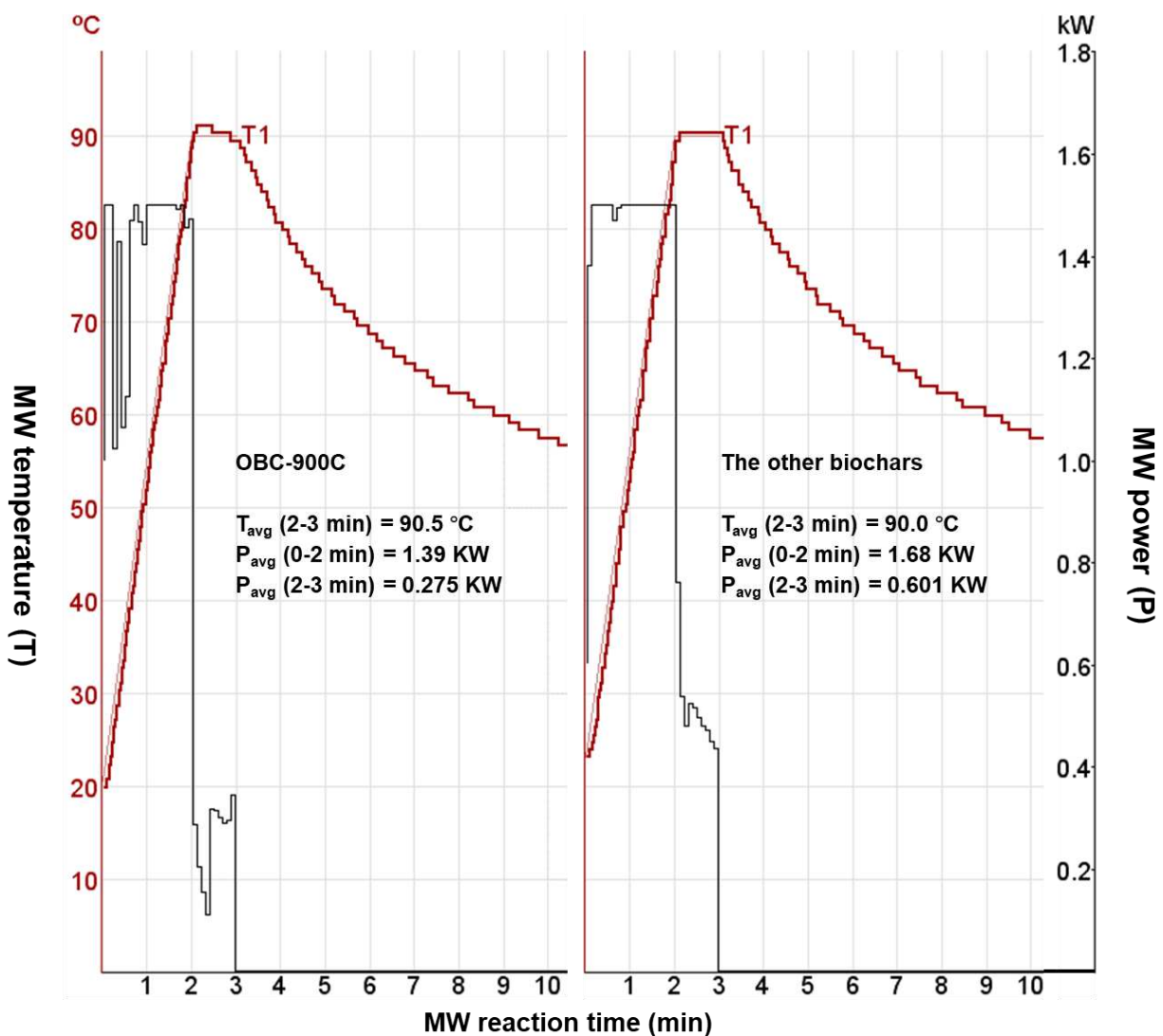
Fig. 6. Temperature and power of the microwave (MW) reactor containing the OBC-900 or the other three biochars (Reaction conditions: 2,4-D $= 100$ mg L^{-1}, biochar $= 1$ g L^{-1}, and $V_{solution} = 20$ mL; MW: temperature increased from 23 ± 2 °C to 90 °C in 2 min and hold for 1 min, $MW_{max} = 1500$W).
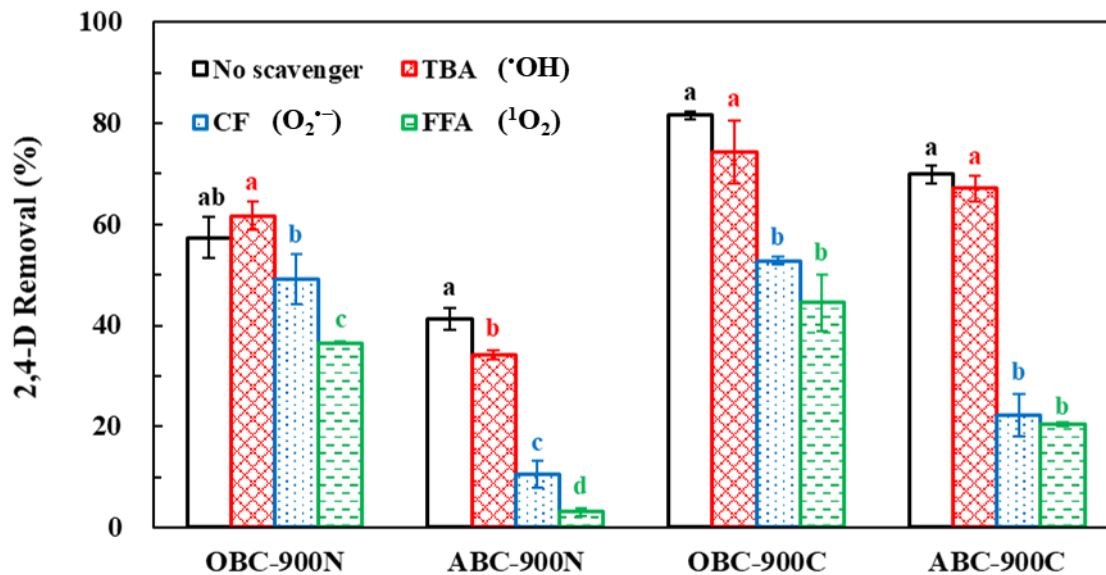
Fig.7. Effect of different radical scavengers on the 2,4-D removal efficiency of various biochars after 1-min reaction in the microwave (MW) system (Reaction conditions: 2,4-D = 100 mg L^{-1} (0.452 mmol), biochar = 1 g L^{-1}, TBA = CF = FFA = 45.2 mmol, $V_{solution}$ = 20 mL, and n = 3; MW: temperature increased from 23 ±2 °C to 90 °C in 2 min and hold for 1 min, MW_{max} = 1500W) (lower-case letters indicate the significance levels ($p < 0.05$) of differences in the results of the same biochar).
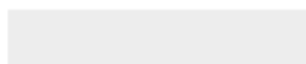
Fig. 8. Reusability of the OBC-900N and OBC-900C for 2,4-D removal after 1-min reaction in microwave (MW) system (Reaction conditions: 2,4-D = 100 mg L^{-1}, biochar = 1 g L^{-1}, V$_{solution}$ = 20 mL, and n=3; MW: temperature increased from 23 ±2 °C to 90 °C in 2 min and hold for 1 min, MW$_{max}$ = 1500W).

SI
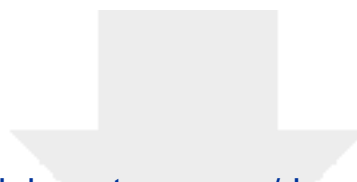
Click here to access/download

Supplementary Material

CEJ_MW-Biochar_2,4-D_SI.docx

Declaration of interests

☒ The authors declare that they have no known competing financial interests or personal relationships that could have appeared to influence the work reported in this paper.

☐The authors declare the following financial interests/personal relationships which may be considered as potential competing interests: